Southern Flow Corridor effectiveness monitoring, 2015-2017: Blue carbon and sediment accretion

See page 2 for photo captions

December 2018, rev. 1

Prepared by:
Laura S. Brophy[1,3], Erin K. Peck[3], Scott J. Bailey[2], Craig E. Cornu[1], Robert A. Wheatcroft[3], Laura A. Brown[4], and Michael J. Ewald[4]

[1] Estuary Technical Group, Institute for Applied Ecology, Corvallis, Oregon, USA
[2] Tillamook Estuaries Partnership, Garibaldi, Oregon, USA
[3] College of Earth, Ocean, and Atmospheric Sciences, Oregon State University, Corvallis, Oregon, USA
[4] Formerly with the Estuary Technical Group; see page 2 for current institutional affiliation

Prepared for:
Tillamook County, Tillamook, Oregon, USA
Tillamook Estuaries Partnership, Garibaldi, Oregon, USA

Funded by the National Oceanic and Atmospheric Administration and U.S. Fish and Wildlife Service.

Southern Flow Corridor effectiveness monitoring, 2015-2017: Sediment accretion and blue carbon

Authors and current institutional affiliations:
Laura S. Brophy[1, 3], Erin K. Peck[3], Scott J. Bailey[2], Craig E. Cornu[1], Robert A. Wheatcroft[3], Laura A. Brown[4], and Michael J. Ewald[5]

[1] Estuary Technical Group, Institute for Applied Ecology, Corvallis, Oregon, USA
[2] Tillamook Estuaries Partnership, Garibaldi, Oregon, USA
[3] College of Earth, Ocean, and Atmospheric Sciences, Oregon State University, Corvallis, Oregon, USA
[4] Benton Soil and Water Conservation District, Corvallis, Oregon, USA
[5] GeomaticsResearch, LLC, Everett, Washington, USA

Contact information for lead author:
Laura Brophy
Director, Estuary Technical Group
Institute for Applied Ecology
563 SW Jefferson Ave., Corvallis, Oregon 97333 USA
brophyonline@gmail.com, (541) 752-7671

Recommended citation:
Brophy, L.S., E.K. Peck, S.J. Bailey, C.E. Cornu, R.A. Wheatcroft, L.A. Brown, and M.J. Ewald. 2018. Southern Flow Corridor effectiveness monitoring, 2015-2017: Sediment accretion and blue carbon. Prepared for Tillamook County and the Tillamook Estuaries Partnership, Tillamook, Oregon, USA. Corvallis, Oregon, USA: Institute for Applied Ecology.

Cover photos. Photo 1: Laura Brown (L) hammers a carbon core at the Goose Point reference site, while Michael Ewald (R) observes. **Photo 2.** L to R: Erin Peck, Michael Ewald, Jake Turner, Laura Brown and Guy Banner extract a "blue carbon" core and measure elevation at the Goose Point scrub-shrub tidal swamp. **Photo 3.** Scott Bailey explores the South Zone of the Southern Flow Corridor site during early post-restoration reconnaissance. **Photo 4.** Ian Rodgers (L) collects a cryocore from a marker horizon plot while Scott Bailey (R) records data.

Data availability: Data from this project are available from the lead author. The carbon cores collected during this study are stored within the Oregon State University Marine Geology Repository's core storage facility and are available for study by others.

Acknowledgments. We are grateful to the following for their major contributions to this project:

- The U.S. Environmental Protection Agency, Coastal Ecology Branch, Newport, Oregon for training on the use of cryocore equipment, and loan of the cryocore equipment;
- Ron Rehn and Chris Knutsen of Oregon Department of Fish and Wildlife's Tillamook North Coast Watershed District Office, and Greg Hublou, for boat assistance during field work;
- Chad Allen for valued assistance with field activities and equipment;
- Guy Banner, Patrick Hayden, and Jake Turner for field assistance with blue carbon core sampling; and Ian Rodger, Anne Matthews, and Philip Matthews for field assistance with feldspar marker horizon and sediment stake sampling.

Revision history:

- Rev. 1 (1/25/19): corrected sentence, p. 37: "This quantity of potential carbon storage (27,000 t C_{org}) is equivalent to the greenhouse gas emissions from about 21,000 passenger cars being driven for a year at average vehicle mileage (EPA 2018)."

Table of contents

Project overview

This report provides the results of ecosystem restoration effectiveness monitoring conducted during 2015-2017 at the Southern Flow Corridor Landowner Preferred Alternative (hereafter, "SFC") project site and reference sites by our team (authors and institutions listed on page 2). The SFC site is located in the Tillamook Bay estuary on the northern Oregon coast, USA (Map 1, Appendix 1); the project's goals include flood reduction and habitat restoration and conservation (Tillamook County 2013). Effectiveness monitoring was designed and implemented to enable the evaluation of progress towards these goals and towards improved ecological functions. The overall monitoring program is described in the SFC Effectiveness Monitoring Plan (Brophy and van de Wetering 2014), available at the Tillamook Oregon Solutions website (https://tillamookoregonsolutions.com/). In addition to the monitoring described in this report, other monitoring conducted by our team at the SFC site and reference sites includes baseline monitoring conducted during 2013-2014 and reported in Brown et al. (2016); and year 2 post-restoration monitoring, currently underway during 2017-2018.

This report describes two main monitoring activities: 1) measurements of sediment accretion using feldspar marker horizon plots and sediment stakes, and 2) collection of deep soil cores to determine "blue carbon" sequestration rates. These activities spanned the period of restoration construction at the SFC site. "Blue carbon" cores were collected in spring 2015, while the site was still diked (i.e. before the site's dikes and tide gates were removed in fall 2016). Sediment accretion (feldspar marker horizon method) was monitored in spring 2017, about 6 months after dike and tide gate removal and restoration of tidal flows. Because the feldspar marker horizon plots were established in 2013 (Brown et al. 2016), the 2017 sediment accretion data reflected sediment deposited during both the pre-restoration period and the post-restoration period. The "blue carbon" cores represented long-term sediment accumulation and carbon sequestration, covering time periods ranging from 30-150 yr prior to the date of sampling in 2015 -- thus many cores spanned the era prior to diking at the SFC site, as well as the diked agricultural period.

Detailed information on sample design and analysis is provided in the SFC Effectiveness Monitoring Plan (Brophy and van de Wetering 2014). Briefly, study sites for this project included the SFC restoration site and three least-disturbed reference sites: Dry Stocking Island, Bay Marsh, and Goose

Point (Map 1, Appendix 1). Within each site, a stratified random sample design was employed. Elevation is often used to stratify sampling in tidal wetlands (Simenstad et al. 1991), and this stratification method was used at the reference sites. However, elevation is relatively homogeneous across the SFC site, whereas land use history varied across the site. Therefore, sampling of the SFC site was stratified into monitoring zones reflecting land use history rather than elevation (Map 2, Appendix 1).

To maximize interpretive power, effectiveness monitoring at the SFC site and reference sites involves measurement of multiple parameters at combined vegetation/physical drivers sample stations. All monitoring described in this report, including feldspar marker horizon plots and "blue carbon" cores, was located at these sample stations.

Terminology and units of measurement

Below, we provide definitions for some terms used in this report. Although some of these may have been used differently by different authors, our goal is to use terminology consistent with other recent and current investigations in our region.

- **"Blue carbon"** refers to carbon stored and sequestered in coastal ecosystems such as mangroves, seagrass beds, and tidal wetlands – including tidal marsh, scrub-shrub tidal wetlands, and forested tidal wetlands of the Pacific Northwest. Most of this carbon is stored in the soils of these wetlands.
- **"Sediment accumulation"** and **"sediment accretion"** are used interchangeably; both refer to sediment deposited on top of the land surface. The rate of accumulation is expressed in this report as the thickness of sediment deposited per year (e.g. 3 mm/yr).
- **"Mass accumulation"** refers to the quantity (mass) of sediment deposited; the rate of accumulation is expressed in this report as mass per unit area per year (e.g. 1 kg/m^2/yr).
- **"Soil carbon density"** refers to the quantity (mass) of organic carbon per unit volume of soil; it is expressed here as mass of carbon per unit of soil volume (e.g. 0.03 g C_{org}/cm^3).
- **"Carbon sequestration"** and **"carbon accumulation"** are used interchangeably; both refer to carbon that is captured and stored over the long term, calculated as the product of sediment carbon density and long-term accretion rate. The rate of sequestration is expressed in this report as the mass of organic carbon stored per unit area per year (e.g. 100 g C_{org}/m^2/yr).
- **"Soil carbon stock"** refers to the total quantity of organic carbon stored in the soil. It is expressed in this report as the mass of soil carbon per unit area (e.g. 400 t C_{org}/ha).
- **Units of measurement** use the metric system and are reported using standard abbreviations, such as "mm" (millimeter), "cm" (centimeter), "m" (meter), "kg" (kilogram), "t" (metric ton or 1000 kg), and "ha" (hectare). Year is abbreviated "yr".

Key findings

To jump to the relevant section, click on the hyperlink (underlined text). Use the back arrow to return to the key findings section.

Sediment accretion (short term) from feldspar marker horizon plots

- At the SFC site, the sediment accretion rate was higher after restoration (in 2017) compared to before restoration in 2014. This was not true at the least-disturbed reference sites, suggesting that restoration led to an increase in accretion at the SFC site.
- Sediment accretion rate was higher – more than double -- for the SFC site (13.8 mm/yr) compared to the reference sites (5.7 mm/yr). This was consistent with our 2014 findings.
- Accretion was higher in low marsh (12.3 mm/yr) than in high marsh (7.3 mm/yr).
- Sediment accretion rates at the SFC site and reference sites were considerably higher than past sea level rise rates in the Tillamook area, estimated at 1.8 mm/yr by Peck (2017), so these sites appear to be maintaining their elevations relative to sea level.

Sediment accumulation (long term) and "blue carbon" sequestration (carbon cores)

- This study -- and associated publications by our team -- provide the first published data on field measurements of carbon stocks and carbon sequestration in Oregon tidal wetlands, helping to fill a major data gap.
- Over time, restoration of the SFC site has the potential to store about 200 tons of organic carbon per hectare, or a total of 27,000 tons of carbon -- equivalent to 100,000 tons of CO_2. Past soil carbon losses from the SFC site due to diking and drainage are estimated to be the same.
- Potential carbon storage in soils of the SFC site after restoration is equivalent to the carbon emissions from about 21,000 passenger cars being driven for a year (average vehicle mileage).
- Sediment accretion at the SFC site (mean = 4.1 mm/yr) and at high marsh and scrub-shrub tidal swamp reference sites (mean = 2.2 mm/yr) has kept pace with past sea level rise.
- Sediment accumulation rates at the low marsh reference cores (10 to >18 mm/yr) were much higher than at the SFC site or the high marsh and shrub swamp reference sites, illustrating the likely resilience of Tillamook Bay tidal wetlands under climate change and sea level rise scenarios.
- Soil carbon stocks were similar at the SFC restoration site and the Dry Stocking Island and Bay Marsh reference sites, ranging from 253 to 484 t C/ha.
- Soil carbon stocks at the Goose Point reference site (860-953 t C/ha) were very high -- about twice the stocks at the SFC site and the Dry Stocking Island and Bay marsh reference sites. In addition, Goose Point soils showed high carbon content in deep soil layers (to 2.6 m depth). These data indicate the importance of conserving least-disturbed tidal wetlands to protect their high level of function for carbon storage.
- The scrub-shrub tidal swamp at Goose Point showed surface soil organic content two to three times higher than the nearby high marsh, indicating the potential importance of this habitat class for carbon sequestration functions.
- The highest carbon sequestration rates in the project were seen at the low marsh reference sites (260 to >420 g $C/m^2/yr$); these were much higher than the global average rate (91 g $C/m^2/yr$, from IPCC 2014).
- Carbon sequestration rates at the SFC site (mean = 150 g $C/m^2/yr$) and the high marsh and scrub-shrub reference sites (85 g $C/m^2/yr$) were similar to global rates (91 g $C/m^2/yr$, from IPCC 2014).

- The different rates of carbon sequestration at the SFC site and reference sites appeared to be driven primarily by site elevation and resulting sediment deposition rates.
- Mean soil carbon densities were similar at the SFC site (0.034 g C/cm^3) and reference sites (0.031 g C/cm^3); these were also similar to the global mean of 0.039 g/cm^3 for tidal wetlands published by Chmura et al. (2003).
- Interestingly, despite diking, carbon sequestration rates at the SFC site were higher during recent periods (last 30-60 years) compared to earlier historical periods, primarily as a result of the higher recent sediment accumulation rates (bullet points above)
- A formula was derived for converting soil organic matter content to elemental carbon content of the soil. This formula is appropriate for use in other northern Oregon tidal wetlands.
- Dry bulk density was strongly correlated with the lightness/darkness (gray scale value) of the CT scan, providing a useful tool for understanding soil physical characteristics.

Lessons learned

Sediment accretion (feldspar marker horizon plots)

- At many locations, dense vegetation (especially the thick reed canarygrass root mat) appears to have prevented formation of a coherent feldspar layer. This has become more apparent over time, and we are concerned that this phenomenon may limit the usefulness of the 2013 marker horizon plots at this site in future years. Establishment of new plots is recommended.
- As we observed in 2014, the sediment stake method did not produce useful results (due to excessive variability), and we recommend this method be discontinued for this project. This may also relate to the type of vegetation at the SFC site (particularly reed canarygrass).

Sediment accumulation and "blue carbon" sequestration (carbon cores)

- Collecting carbon cores from reference sites as well as the SFC site was vital to development of key findings, such as prediction of the quantity of carbon that could be stored following restoration.
- Due to the large variability in recent sediment accumulation and carbon sequestration rates within the SFC site, we recommend future studies increase the number of samples within the SFC site.
- Although the lead 210 (^{210}Pb) method is not commonly used in diked former tidal wetlands, it appeared to produce good results at the SFC site and may therefore be appropriate for future studies in diked wetlands.
- Cesium 137 (^{137}Cs) methods had some limitations for this study due to possible post-depositional remobilization. However, this method worked well for cores with very rapid sediment accumulation rates, where the ^{210}Pb method did not work well. Therefore, the two methods were complementary, and both methods were needed for good results.

Section 1. Sediment accretion (feldspar marker horizon plots)

This section provides results of sediment accretion monitoring using feldspar marker horizon plots at the SFC site and reference sites, based on data collected during spring 2017 and previous work in 2013 and 2014. As noted in the baseline monitoring report, sediment accretion (or erosion) affects plant community establishment, habitat development and resilience to climate change. This study was designed to:

- Quantify changes in vertical sediment accretion (or erosion) after project implementation;
- Determine how sediment accretion rates at the project site compare to projected rates of sea level rise; and
- Help interpret data from other monitored parameters including plant communities, fish populations, and water quality.

We established marker horizon sampling plots and sediment stakes (another method for measuring accretion or erosion) in 2013, prior to restoration activities, at 27 locations within the SFC restoration site, and at 11 locations within the 3 least-disturbed reference sites. When combined, the marker horizon and sediment stake sampling methods can detect accretion or erosion, but since no erosion was observed, we will refer to the plots as "sediment accretion plots" for simplicity in this report.

We sampled the marker horizon plots and sediment stakes during fall 2014 and again during spring 2017. The 2017 sampling effort occurred approximately 6 months after completion of the bulk of the SFC restoration construction efforts, so as noted above, 2017 data from those plots reflected sediment deposited during both the pre-restoration period (3 yr) and the post-restoration period (6 mo).

This section describes: 1) sediment accretion sampling and analysis methods; 2) results from 2017 sampling (first post-restoration construction sampling period); and 3) comparisons with sediment accretion data in the SFC baseline monitoring report (Brown et al. 2016).

Methods

Sample design for sediment accretion is described in the SFC Effectiveness Monitoring Plan (Brophy and van de Wetering 2014) and the SFC baseline monitoring report (Brown et al. 2016). Sediment accretion/erosion monitoring at the SFC site and nearby reference marshes used two methods: 1) feldspar marker horizon plots sampled using cryocoring methods (Cahoon and Turner 1989, Callaway et al. 2013); and 2) sediment stakes (Roegner et al. 2008). Sections below describe these methods in further detail. Feldspar plots and sediment stakes were established adjacent to one another to allow direct comparison between the two methods. Sediment accretion monitoring plots were marked with tall (3 m) PVC poles to facilitate relocation in tall vegetation and to help prevent disturbance during farming and restoration construction. Thirty-eight plots (27 restoration, 11 reference) were established in fall 2013 using a stratified random sample design as described in the SFC Effectiveness Monitoring Plan (Brophy and van de Wetering 2014). Plot locations are shown in Maps 3, 5 and 7 (Appendix 1).

We sampled all feldspar plots and sediment stakes after one year (November 2014), yielding baseline annual accretion rates at SFC and reference sites. We resampled 32 of the 38 the plots during April 2017 (representing about 3 years pre-restoration and 6 months post-restoration), and compared results to baseline data. Five of the 2013 plots were not resampled in 2017 because they were inaccessible within

time constraints, or were damaged by farm machinery or large woody debris (2017 elevation shown as "Not sampled" in Table 1). The location and elevation of each plot was recorded in October 2013 using high-precision RTK GPS/GNSS survey instruments (Table 1). During both the November 2014 and April 2017 sampling efforts, we again used a high-precision RTK GPS/GNSS instrument to re-measure elevations at each plot, although we were unable to obtain GPS data at two locations (2017 elevation shown as "Not available" in Table 1). Table 1 includes UTM coordinates for each plot, and elevations from both 2013 and 2017. The spatial reference system for these measurements is provided in Appendix 2.

Table 1. Locations (m UTM Zone 10N, NAD83) and elevations (m NAVD88 Geoid 12A) of all sediment accretion plots at the SFC site and reference sites. Elevation columns show which plots were monitored each year; for 2017, "Not available" indicates the plot was sampled, but RTK-GPS data could not be obtained. Habitat types: LM = low marsh, HM = high marsh.

	Zone	Plot	Easting (m)	Northing (m)	2013 Elevation (m)	2017 Elevation (m)	Habitat Type
SFC site	North	A01	431451	5036408	2.17	Not available	LM
		A02	431464	5036523	2.54	2.59	HM
		A03	431687	5036400	2.29	Not available	LM
		A04	431483	5036429	2.19	2.14	LM
		A05	431951	5036225	2.28	2.30	LM
	Middle	A09	431669	5035880	1.87	1.84	LM
		A10	431365	5036167	2.02	2.05	LM
		A11	431792	5035853	1.91	1.95	LM
		A12	431395	5036171	1.93	1.93	LM
		A13	431338	5035887	1.98	1.94	LM
		A14	431070	5035987	2.02	2.02	LM
		A15	431705	5036007	1.96	Not sampled	LM
		A16	431083	5036141	1.96	1.98	LM
		A17	430369	5036305	2.04	2.03	LM
	South - no crop	A37	430562	5035992	1.94	2.00	LM
	South - crop	A25	431245	5035870	1.79	Not sampled	LM
		A26	431510	5035722	1.69	Not sampled	LM
		A27	431024	5035828	1.79	Not sampled	LM
		A28	431375	5035708	1.94	1.96	LM
		A29	431266	5035774	1.79	Not sampled	LM
		A30	431667	5035523	1.94	2.02	LM
		A31	430926	5035941	1.98	1.98	LM
		A72	431912	5035478	2.27	2.30	LM
		A73	431942	5035413	2.39	2.39	HM
		A74	432001	5035358	2.42	2.42	HM
	Nolan - ungrazed	A75	432299	5035367	2.17	2.20	LM
		A77	432277	5035337	2.11	2.12	LM
Reference sites	Bay Marsh	A62	430131	5036711	2.18	2.23	LM
		A63	430016	5036969	2.12	2.20	LM
		A64	430164	5036812	2.13	2.36	LM
	Dry Stocking Island-low marsh	A46	430794	5035523	1.96	1.99	LM
		A47	430806	5035438	2.00	2.07	LM
	Dry Stocking Island-high marsh	A40	431377	5035372	2.68	2.68	HM
		A41	431526	5035387	3.05	3.09	HM
		A42	431077	5035374	2.62	2.59	HM
		A43	431174	5035388	2.63	2.61	HM
	Goose Point	A68	430963	5039940	2.65	2.62	HM
		A69	430952	5039899	2.69	2.67	HM

Feldspar marker horizon method

White feldspar powder is used as a soil horizon marker because it contrasts sharply with dark wetland soils (Cahoon et al. 2000). In November 2013, we spread a 5-15 mm layer of feldspar over a 0.25 m^2 area in the center of a larger demarcated plot (1 m^2). We marked the corners of the 1 m^2 plot with 13 mm (½ in) diameter PVC stakes. One corner stake was originally painted orange, then capped in 2017 with a PVC elbow (as the paint had faded) to mark a consistent starting point for determining sample coordinates. One year (November 2014) later and approximately 3.4 years (April 2017) later, we returned to the plots with a pressurized canister or "Dewar" of liquid nitrogen and associated cryocoring probe. We used the liquid nitrogen-filled probe to freeze and extract a minimum of two sample cores from each feldspar plot (Cahoon et al. 1996) (Figure 1). We measured the depth of accreted material above the feldspar horizon for each core (distance from the top of soil surface to top of feldspar layer) up to four times per core depending on how well defined the feldspar layer was (Figures 2 - 4). As in previous sampling efforts, we recorded the X-Y coordinates of each core within the feldspar patch (with the PVC elbow as the origin) to ensure that specific core location would not be re-sampled in future years of monitoring. In addition, after taking measurements we returned each core (with feldspar removed) to its initial location in the ground.

In a few locations, as necessitated by field logistics and liquid nitrogen supply, we used a sharp knife to extract a core instead of cryocoring. Although potentially less accurate, the knife core results were generally similar to the cryocore results, so we included them in the dataset.

Figure 1. Field crew collecting cryocore at a feldspar marker horizon plot. Liquid nitrogen is injected into the ground through a small copper tube, which creates the frozen core that is removed for measurement (Figures 2-4).

Figure 2. Example of field photo showing a feldspar marker horizon core and its sample number. This core shows an excellent quality feldspar layer. A photo like this was taken of each core, for archival purposes. Sediment to the left of the white feldspar horizon has been deposited since the feldspar layer was placed in 2013.

Figure 3. Example of field photo showing a feldspar marker horizon core with an incomplete or low-quality feldspar layer. Cryocores of this and lesser quality were common in areas dominated by reed canarygrass.

Figure 4. Example of field photo showing a feldspar marker horizon core with no visible feldspar layer. Cryocores lacking a visible feldspar layer typically occurred in areas dominated by reed canarygrass.

Sediment stake method

In November 2013, we established a sediment stake plot adjacent to each feldspar marker horizon plot. For these plots, we drove two 1 m sections of 2.5 cm diameter Schedule 80 PVC pipe (gray) deeply into the ground 1 m apart until the tops were level with one another. We determined the distance from the tops of the stakes to the soil surface by laying a meter stick horizontally and measuring vertically to the ground surface at 10 cm intervals between the stakes. We used the interior eight measurements to calculate a mean and standard error for a "distance to soil surface" measurement at each sediment stake plot. In November 2014 (one year later) and April 2017 (approximately 3.4 years later), we repeated this method. We calculated the difference between means for each sample date to obtain the accretion or erosion rate (mm/yr) for each plot. Erosion was indicated when the difference between the measurements was negative, and accretion was indicated when the difference between the measurements was positive. Sediment stakes were not intended to provide precise measurements of small changes in sediment accretion, but rather to provide back-up and validation for the feldspar plot measurements. For example, sediment stakes could indicate erosion, which is not measurable using the feldspar method; or sediment stakes could corroborate accretion rates measured in the feldspar plots. However, in 2017 (just as in 2014), challenges in applying the sediment stake method prevented the use of the data, so we recommend discontinuing this method in future years (see "**Accretion sampling challenges**" below).

Accretion sampling challenges

Dense vegetation at many sample plots – particularly reed canarygrass -- adversely affected our use of the feldspar marker horizon technique. During our spring 2017 field effort, the feldspar horizon was absent or of very poor quality in cryocores from five plots ("PQ" in Table 2; see example in Figure 4); in many other cases, the feldspar layer was discontinuous, reducing the number of replicate

measurements taken – in one case (plot A12), to just a single measurement (Figure 3). We suspect that the dense reed canarygrass dense root mat sometimes prevented the feldspar from forming a coherent layer. While we were able to detect at least some feldspar in nearly all the cryocores in 2017, we are concerned that time (and decomposition of the root mat) will exacerbate this issue and may limit the usefulness of the 2013 marker horizon plots at the SFC site in future years. Establishment of new plots at the SFC site is recommended to allow continuation of the study. Although the new plots should be randomly placed (consistent with the overall monitoring design), some plots should be placed in areas where reed canarygrass has died back, to improve the chances of a coherent feldspar layer.

We found substantial variability and inconsistencies in the sediment stake data from 2013, 2014 and 2017, confirming the challenges described for this method in the baseline monitoring report (Brown et al. 2016). These inconsistent results are probably due to the difficulty of precisely determining the wetland ground surface within the dominant vegetation at the SFC site (primarily reed canarygrass). Reed canarygrass forms a dense aboveground root mat of highly variable thickness, making it difficult to consistently define the soil surface. While the sediment stake method may work well on mudflats, in less dense plant communities, or in dense communities of other species, it has not worked well in the reed canarygrass-dominated portions of the SFC site. Since the method did not work well in either 2014 or 2017, we recommend this method be discontinued, and we did not use the sediment stake data in preparing this report. This decision follows the baseline monitoring report's recommendation that data from the feldspar marker horizon method, rather than the sediment stake method, should be used to compare accretion rates between the SFC site and the reference sites (Brown et al. 2016).

Data analysis

Measurements from the marker horizon plots were converted to annual accretion rates by dividing the total measured accretion by the number of years between plot establishment (October 2013) and April 2017 sampling (3.5 years). Statistical analysis was conducted using VassarStats (http://vassarstats.net/) and Microsoft Excel. We calculated descriptive statistics (mean, standard error) for marker horizon data. We used two-tailed t-tests to compare accretion rates between the SFC site and reference sites. We found inconsistencies in the way that feldspar marker horizon data were handled in 2014, so we corrected the 2014 data and ran a two-tailed test (assuming unequal variances) comparing restoration to reference annual accretion rates for 2014. The data corrections made only a small difference in the mean rates, but the t-test showed different results from the analysis run in 2014 (see "**Results**" below).

We used two methods to investigate the relationship between sediment accretion rates and wetland surface elevation (elevation obtained using RTK-GPS equipment): 1) we ran a simple linear regression on accretion rate versus elevation; and 2) we categorized plots into low or high marsh and ran a two-way ANOVA comparing accretion rates by low versus high marsh and by treatment (restoration, i.e. the SFC site, versus reference sites). We classified plots as low or high marsh by relating plot elevations to the Mean Higher High Water (MHHW) tidal datum, which was 2.4 m NAVD88 based on local water level analysis (Brown et al. 2016). Plots below 2.4 m NAVD88 (i.e., below MHHW) were classified as low marsh, and plots above 2.4 m NAVD88 were classified as high marsh. However, Plot A73 was grouped with high marsh rather than low marsh, because it was just 1 cm below MHHW -- much higher than the other low marsh plots in the study.

To assess whether accretion rates have changed since completion of restoration construction at the SFC site, we also ran a two-way ANOVA comparing rates by treatment (restoration versus reference) and

year (2014 versus 2017). However, this analysis is not completely orthogonal (that is, the two factors are not statistically independent), because restoration occurred partway through the 2014-2017 sampling interval. Therefore, we also conducted a more conservative analysis using two-tailed t-tests to compare accretion rates between 2014 and 2017 at the restoration site, and between 2014 and 2017 at the reference sites.

For purposes of this analysis, as in 2014, we grouped sediment accretion plots in the "Nolan crop" zone and the "South crop" zones because they probably had similar depositional environments. We hoped to replicate all analyses employed in the SFC baseline report (Brown et al. 2016) and use a one-way ANOVA to compare accretion among zones. However, several zones had too few sample plots in 2017 for such an analysis, so we did not conduct this test. However, we do provide average accretion rates by zone below.

Results and discussion

This section provides the results of 2017 sediment accretion/erosion monitoring at the SFC site and reference sites, and compares these findings to baseline data from the same sites, and to data from other tidal wetlands. Table 2 provides mean annual feldspar marker horizon sediment accretion rates for each plot sampled during 2014 and 2017.

Table 2. Annual sediment accretion rates (mean ± 1 SE) for plots at reference sites and within the Southern Flow Corridor project site during 2014 and 2017. In the accretion rate columns, "NS" indicates the plot was not sampled; "PQ" indicates missing data due to a poor quality feldspar layer (see "**Methods**" above for details).

	Zone	Plot	2014 Data Annual Accretion (mm/yr)	2017 Data Annual Accretion (mm/yr)
SFC site	North	A01	30.4 ± 5.9	10.2 ± 1.3
		A02	2.9 ± 0.8	16.6 ± 2.0
		A03	3.6 ± 1. 5	7.1 ± 0.6
		A04	31.4 ± 5.7	15.6 ± 2.1
		A05	0.0 ± 0.0	PQ
	Middle	A09	PQ	PQ
		A10	2.7 ± 1.7	PQ
		A11	6.0 ± 1.1	14.1 ± 1.0
		A12	9.9 ± 3.9	16.7*
		A13	0.0 ± 0.0	19.8 ± 1.6
		A14	3.0 ± 2.0	11.0 ± 0.6
		A15	12.4 ± 4.9	NS
		A16	11.8 ± 4.0	15.7 ± 0.4
		A17	9.6 ± 3.0	13.9 ± 2.0

	Zone	Plot	2014 Data Annual Accretion (mm/vr)	2017 Data Annual Accretion (mm/vr)
	South - no crop	A37	10.6 ± 4.2	PQ
	South - crop	A25	3.8 ± 1.2	NS
		A26	1.1 ± 1.1	NS
		A27	6.2 ± 0.8	NS
		A28	7.1 ± 2.2	15.5 ± 0.9
		A29	14.3 ± 3.9	NS
		A30	4.0 ± 1.2	13.5 ± 1.1
		A31	3.5 ± 1.1	11.3 ± 1.0
		A72	1.0 ± 0.7	11.8 ± 0.9
		A73	8.7 ± 2.8	14.8 ± 0.7
		A74	0.9 ± 0.7	11.5 ± 1.5
	Nolan - ungrazed	A75	11.4 ± 2.3	PQ
		A77	1.9 ± 0.8	16.4 ± 1.1
Reference sites	Bay Marsh	A62	7.7 ± 1.7	6.6 ± 0.5
		A63	7.0 ± 0.6	15.2 ± 0.5
		A64	3.2 ± 1.0	6.7 ± 0.9
	Dry Stocking Island-low marsh	A46	1.2 ± 0.7	6.1 ± 0.4
		A47	3.3 ± 0.4	5.7 ± 0.6
	Dry Stocking Island-high marsh	A40	0.4 ± 0.3	3.5 ± 0.3
		A41	0.0 ± 0.0	7.4 ± 1.8
		A42	4.4 ± 0.8	3.2 ± 0.4
		A43	0.4 ± 0.3	2.8 ± 0.2
	Goose Point	A68	1.8 ± 0.6	3.8 ± 0.8
		A69	PQ	2.1 ± 0.3

* For plot A12, only a single measurement could be obtained, so no uncertainty is provided.

Based on our 2017 feldspar marker horizon data, the mean annual accretion rate was significantly greater for the SFC restoration site (13.8 mm/yr) compared to the reference sites (5.7 mm/yr) (Figure 5, Table 3; t = 6.37, df = 26, P <0.0001). This is consistent with the results of our analysis of the 2014 feldspar marker horizon data, for which the mean annual accretion rate was significantly greater for the SFC site (7.9 mm/yr) compared to the reference sites (2.9 mm/yr) (Figure 5, Table 3; t = 2.73, df = 33, P = 0.01).

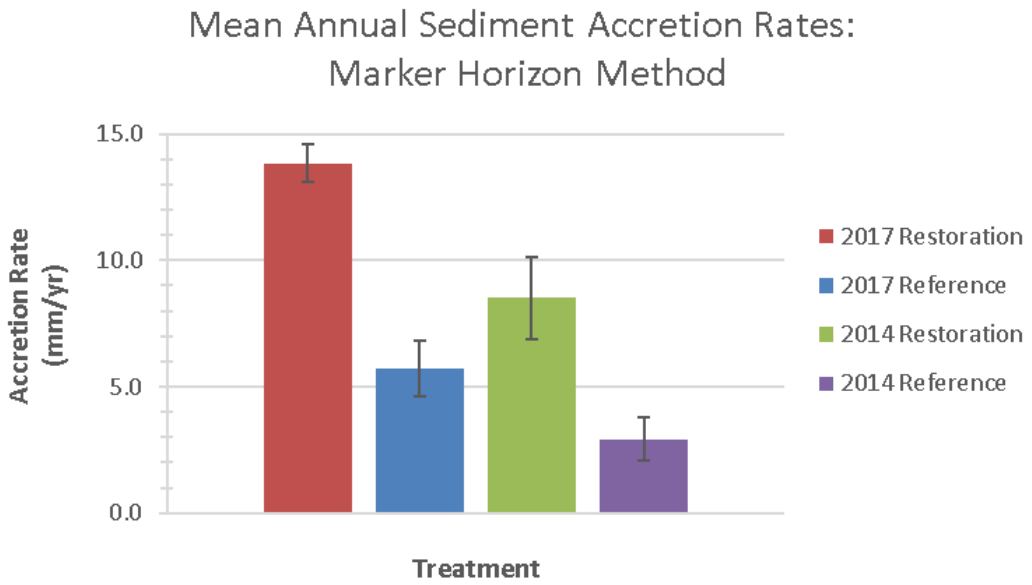

Figure 5. Mean (±1 SE) annual sediment accretion rates for the SFC site and reference sites in 2014 and 2017 using the feldspar marker horizon method.

Table 3. Mean **a**nnual sediment accretion rates (mean ±1 SE) from 2014 and 2017 sampling at SFC (restoration) and reference sites.

	Sediment accretion rate (mm/yr)		
Sample year	**Restoration**	**Reference**	**Mean**
2014	7.93 ± 1.61	2.94 ± 0.87	6.50 ± 1.23
2017	13.84 ± 0.74	5.72 ± 1.09	10.65 ± 0.98
Mean	10.33 ± 1.09	4.40 ± 0.76	8.35 ± 0.85

Two-way ANOVA analyzing accretion rate by year and treatment (restoration vs. reference) showed that the mean annual accretion rate for 2017 (10.7 mm/yr) was significantly greater than for 2014 (6.5 mm/yr) (F = 8.34, P = 0.0054) (Tables 3 and 4). In addition, mean annual accretion was significantly higher for SFC restoration plots (10.3 mm/yr) than for reference plots (4.4 mm/yr) (Tables 3 and 4; F = 15.20, P = 0.0003). However, the interaction effect was not significant (P = 0.0521; Table 4), and no further comparisons (e.g., 2014 reference vs. 2017 reference, 2014 restoration vs. 2017 restoration, etc.) could be made within the ANOVA. T-tests, however, showed that mean annual accretion rates at the SFC restoration site were significantly higher in 2017 (13.8 mm/yr) compared to 2014 (7.9 mm/yr) (t = 3.3, df = 33, P = 0.002), while mean annual accretion rates did not differ significantly between 2017 (5.7 mm/yr) and 2014 (2.9 mm/yr) at the reference sites (t = 2.01, df = 18, P = 0.06). These results strongly suggest that restoration has increased accretion rates at the SFC site.

Table 4. Summary of 2-way ANOVA, year and site treatment (restoration vs. reference), 2014 and 2017 sediment accretion data.

ANOVA Summary					
Source	**SS**	**df**	**MS**	**F**	**P**
Year (2014/2017)	269.38	1	269.38	8.34	0.0054
Treatment (Reference/Restoration)	490.89	1	490.89	15.20	0.0003
Interaction (Year x Treatment)	126.81	1	126.81	3.93	0.0521
Error	1905.9	59	32.30		
Total	2793	62			

Accretion rates are generally understood to be inversely correlated with elevation, with low marsh accreting more rapidly than high marsh (Morris et al. 2002, Chmura et al. 2003). However, simple regression analysis of our 2017 data did not show a significant relationship between elevation and accretion rates within the SFC restoration zone or at reference sites (Figure 6). This is probably due to small sample size and the influence of factors other than elevation that may strongly affect accretion at these sites, such as proximity to rivers that often flood. The baseline (2014) monitoring showed similar results (Brown et al. 2016).

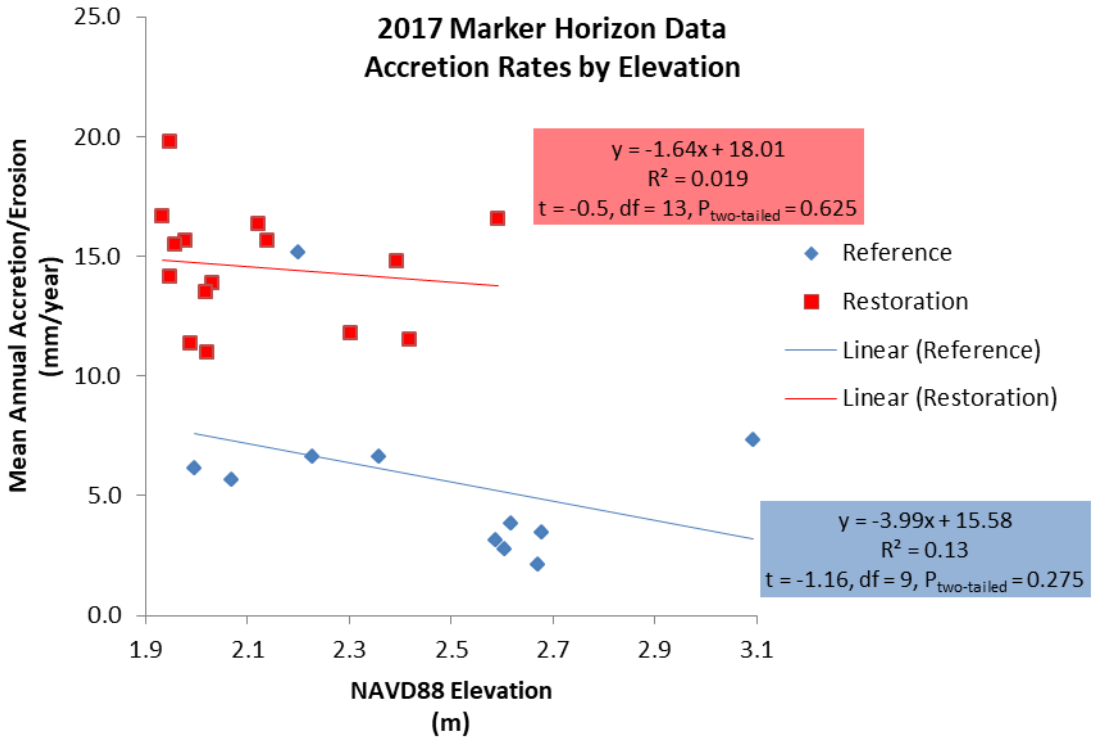

Figure 6. Sediment accretion rates relative to plot elevation for plots at the SFC restoration site and reference sites, based on 2017 marker horizon data.

For the 2017 data, however, a relationship between accretion rate and elevation was detected when plots were classified as low or high marsh and analyzed with two-way ANOVA: the annual accretion

rate was significantly higher in low marsh (12.3 mm/yr) than in high marsh (7.3 mm/yr) (F =15.7, P = 0.0006; Tables 5 and 6). This contrast was driven by the results in reference sites; the mean accretion rate was similar in low and high marsh at the SFC site (Table 5). This result matched expectations and relationships described in the literature (Morris et al. 2002, Chmura et al. 2003); and this result also agreed with our blue carbon analysis (see '**Sediment accumulation and "blue carbon" sequestration (carbon cores)'** below). This ANOVA also corroborated the t-test results above, showing that the annual accretion rate measured in 2017 was higher at the SFC restoration site (13.8 mm/yr) compared to the reference sites (5.7 mm/yr) (F = 45.7, P < 0.0001; Tables 5 and 6).

Table 5. Annual sediment accretion rates from 2017 sampling (mean ±1 SE) at SFC (restoration) and reference sites, by wetland type (low marsh vs. high marsh/scrub-shrub).

	Sediment accretion rate, 2017 data (mm/yr)		
Habitat type	**Restoration**	**Reference**	**Mean**
Low marsh	13.75 ± 0.87	8.05 ± 1.79	12.25 ± 0.97
High marsh	14.27 ± 1.48	3.79 ± 0.75	7.28 ± 1.86
Mean	13.84 ± 0.74	5.72 ± 1.09	10.65 ± 0.98

Table 6. Summary of 2-way ANOVA, habitat type and site treatment (restoration vs. reference), 2017 sediment accretion data.

ANOVA Summary					
Source	**SS**	**Df**	**MS**	**F**	**P**
Habitat (Low Marsh/High Marsh)	150.85	1	150.85	15.65	0.0006
Treatment (Reference/Restoration)	440.50	1	440.50	45.70	<0.0001
Interaction (Habitat x Treatment)	0	1	0	0	1.0
Error	231.34	24	9.64		
Total	722.08	27			

Although we were unable to compare accretion among SFC sample zones with a one-way ANOVA (as described in "**Methods**" above), we did calculate means and standard errors for as many zones as possible to facilitate comparison with pre-restoration results in Brown et al. (2016) (Figure 7). The relationships between zones were generally similar to baseline data (Figure 75 in Brown et al. 2016).

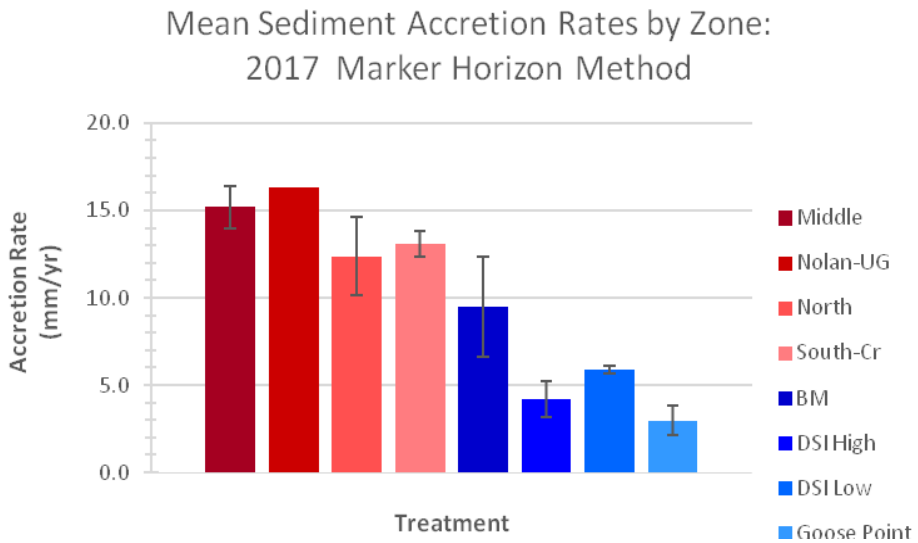

Figure 7. Mean sediment accretion rates among zones at the SFC restoration site (red bars) and four nearby reference sites (blue bars). Error bars indicate 1 standard error. There was only a single plot in Nolan-UG, so descriptive statistics could not be calculated.

Conclusions

Feldspar marker horizon cryocores collected in 2017 contained sediment deposited during both the pre-restoration period and the post-restoration period, so they do not allow separate determination of pre-restoration versus post-restoration accretion rates. However, the significant increase in annual accretion rate at the SFC site from 2017 sampling (compared to 2014 sampling) strongly suggests that restoration of tidal inundation allowed increased accretion compared to pre-restoration conditions.

Even prior to restoration, feldspar plots at the SFC site showed higher rates of accretion than the reference sites (Brown et al. 2016), and this effect was stronger after restoration, as described in this report. The high accretion rates prior to dike removal were probably due in part to the lower elevation of the SFC site compared to the reference sites, but were still surprising because the site was diked. However, these results were corroborated by long-term accretion rates from the "blue carbon" study (see ' Sediment accumulation and “blue carbon" sequestration (carbon cores)" below). The observed high accretion rates at the SFC site during the diked period may have been due to winter floods that overtopped the dikes, carrying sediment onto the site. The rivers that flow into Tillamook Bay surrounding the SFC site carry very large loads of sediment (Pearson 2002, Peck 2017). Removal of the dikes that formerly surrounded the SFC site increases the opportunity for these sediments to be deposited before reaching the bay, which may improve navigation and habitat conditions in the bay.

Sediment accretion at the SFC site and reference sites were considerably higher than past rates of sea level rise in the Tillamook area, estimated at 1.8 mm/yr by Peck (2017), so accretion at these sites appears to be keeping pace with sea level rise. Combined with information on the high sediment supply to the Tillamook Bay estuary (see "**Climate change resilience**" below), this suggests these sites may be resilient in the face of projected sea level rise.

When analyzed by wetland type (low versus high marsh), the feldspar marker horizon data showed

higher accretion in low marsh compared to high marsh – a result that was expected, since accretion rates are generally understood to be strongly (and inversely) tied to elevation (see "**Carbon densities, carbon sequestration rates, and wetland elevation**" below). Other studies have emphasized dramatic differences in accretion rates between low marsh and high marsh habitats, and most tidal wetland development models (e.g. Allen 1990, Morris et al. 2002) and Pacific Northwest observations (Thom 1992, Simenstad and Thom 1996) show higher accretion rates in low marsh compared to high marsh.

Sediment accretion rates measured in feldspar plots at the SFC site and reference sites were, on average, higher than at reference sites in the Siuslaw River estuary of Oregon (Brophy et al. 2015), which averaged around 5.1 mm/yr, and also higher than average rates from other studies of sediment accretion in the PNW (e.g. Thom 1992, Simenstad and Thom 1996, Diefenderfer et al. 2013). These rates may reflect the high sediment inputs into Tillamook Bay, as described above (Pearson 2002).

Sediment accretion within tidal wetlands has been little studied in the Pacific Northwest, and comparisons between diked former tidal wetlands and least-disturbed reference sites have been lacking. Our data help to fill these data gaps, leading to better understanding of tidal wetland physical processes and resilience to climate change.

Section 2. Sediment accumulation and “blue carbon" sequestration (carbon cores)

Background

Tidal wetlands, including emergent marshes, scrub-shrub and forested tidal swamps, and seagrass beds, store or "sequester" carbon -- also referred to as "blue carbon" -- through burial and preservation of organic material in the soil (Mcleod et al. 2011). However, once drained and converted for human land uses such as agriculture, these areas may rapidly release carbon back into the atmosphere and lose their capacity for future carbon burial. The potential for blue carbon sequestration following restoration of disturbed wetlands in the Pacific Northwest is likely high (Crooks et al. 2014). Thus, information on blue carbon sequestration potential at restoration sites is required for policy makers and land-use managers to assess alternative land-use policies. Moreover, measurement of historical carbon sequestration rates at least-disturbed reference sites is needed to estimate the uptake and carbon preservation potential of possible restoration sites. Knowledge of recent and historical carbon sequestration rates in least-disturbed wetlands adds incentive for conservation of these areas. Finally, information on sediment accumulation rates is vital to our understanding of tidal wetland resilience in the face of future climate change and sea level rise.

This study sought to: 1) quantify carbon stocks and carbon sequestration rates at the SFC restoration site and nearby least-disturbed reference sites (Bay Marsh, Dry Stocking Island, and Goose Point); 2) estimate the carbon losses that occurred when the restoration site was diked and drained; 3) predict the post-restoration carbon storage capacity of the restoration site; and 4) gain some understanding of potential tidal wetland resilience to sea level rise in the area.

Methods

Overview

Briefly, soil carbon stocks were calculated by analysis of carbon content and bulk density of sediment within soil cores collected from restoration and reference sites. These are also called "carbon cores" and are the only cores referred to in this section (as opposed to the cryocores described in the previous section). Carbon sequestration rates (also called "carbon accumulation rates" or "CARs") were calculated using the soil carbon density (carbon concentration) data along with sediment accumulation rates (SARs), determined by analyzing radioisotope levels (^{210}Pb and ^{137}Cs) in the carbon cores.

Field sampling

Field sites consisted of the SFC site and the least-disturbed reference sites described in Section 1 (Bay Marsh, Dry Stocking Island and Goose Point). These sites are described in the SFC Effectiveness Monitoring Plan (Brophy and van de Wetering 2014) and the SFC baseline monitoring report (Brown et al. 2016).

Field sampling, conducted in April 2015, was designed to meet three criteria: 1) co-locate blue carbon sampling with vegetation and physical drivers monitoring (to maximize interpretive power); 2) enable

comparisons between restoration and reference sites; and 3) sample across the elevation gradient, including low marsh, high marsh and scrub-shrub tidal swamp reference samples.

At the SFC site, four soil carbon cores were collected, one in each major monitoring zone (North, Middle, South (cropped), and Nolan Slough (cropped) (Map 2, Appendix 1). At the reference sites, two cores were collected in low marsh, three in high marsh, and one in scrub-shrub tidal wetland (also referred to as "scrub-shrub tidal swamp"). The scrub-shrub wetland was located at the Goose Point reference site and was dominated by brackish-tolerant shrubs including black twinberry (*Lonicera involucrata*) and willows (*Salix* spp.). At all sample locations except the scrub-shrub tidal swamp, carbon cores were co-located with combined vegetation/physical drivers monitoring stations described in the SFC Effectiveness Monitoring Plan (Brophy and van de Wetering 2014) and the SFC baseline monitoring report (Brown et al. 2016). Although it fell outside the scope of other SFC project monitoring, the Goose Point scrub-shrub tidal swamp core was added because data on this habitat class are very sparse, and because it could contribute substantially to our team's other studies across the tidal-marsh-to-tidal-swamp gradient (Brophy 2009, Brophy et al. 2011, Brophy et al. 2017, Peck 2017).

Cores were either short (1.5 m in length) or long (3 m in length). To obtain the cores, PVC pipe 10 cm in diameter and 1.5 or 3 m in length was pounded into the ground using a sledgehammer and retrieved using a truck jack. The location and sediment surface elevation at each core was recorded using high-precision RTK GPS/GNSS survey instruments; the spatial reference system used is described in Appendix 2. In the field, each long core was cut into two ~1.5 m sections using a pipe cutter. These sections were stored within the Oregon State University (OSU) Marine Geology Repository's refrigerated core storage facility, where they will be maintained indefinitely and are available for study by others.

Carbon core identification codes (Table 7) were assigned to each core, with the last two digits of the ID code corresponding to the nearby combined vegetation/physical drivers monitoring station (Brown et al. 2016). For example, Core ID# DSI-H.A043 corresponds to monitoring station A043, and Core ID# NOR-SAM.A004 corresponds to monitoring station A004.

Core types (short or long), habitat types, and UTM coordinates are shown in Table 7; core locations are shown in Maps 4, 6, and 8 (Appendix 1).

Table 7. Locations and elevation data for carbon cores at the SFC site and reference sites. Easting and Northing represent UTM Zone 10 N coordinates in meters (NAD83 datum). Elevations are expressed in meters NAVD88 (Geoid 12A). Locations are shown in Maps 4, 6 and 8 (Appendix 1). See Appendix 2 for spatial reference system information.

Site type	Wetland zone or site name	Core location	Core type	Wetland type	Core ID	Easting (m)	Northing (m)	Soil surface elevation (m)	Local MHHW (m)*
SFC (restoration)	Middle zone	A009	short	Diked pasture	MID.A009	431672	5035883	1.86	2.44
	North zone	A004	short	Diked pasture	NOR-SAM.A004	431479	5036430	2.22	2.44
	Nolan crop	A073	short	Diked pasture	NS-CR.A073	431941	5035419	2.37	2.44
	South zone crop	A028	short	Diked pasture	SO.CR.A028	431378	5035704	2.01	2.44
Reference	Bay Marsh	A063	short	Emergent tidal wetland (low marsh)	BM.A063	430016	5036970	2.12	2.37
	Bay Marsh	A064	long	Emergent tidal wetland (high marsh)	BM.A064	430164	5036813	2.31	2.37
	Dry Stocking Island high marsh	A043	long	Emergent tidal wetland (high marsh)	DSI-H.A043	431171	5035388	2.61	2.44
	Dry Stocking Island low marsh	A047	short	Emergent tidal wetland (low marsh)	DSI-L.A047	430806	5035439	2.00	2.44
	Goose Point	A068	long	Emergent tidal wetland (high marsh)	GP.A068	430963	5039939	2.66	2.39
	Goose Point	Shrub	long	Scrub-shrub tidal wetland (tidal swamp)	GP.W	430959	5040017	2.74	2.39

* Local MHHW was calculated from local water level data collected during baseline monitoring; see Figure 13 in Brown et al. (2016).

Laboratory analyses

Soon after collection, all core sections were scanned using a Computerized Tomography (CT) system at the OSU College of Veterinary Medicine. CT imaging provides high-resolution views of sediment stratigraphy (e.g. changes in texture, presence of root mats), and CT images can be used to estimate sediment bulk density. Each core was split in half lengthwise, exposing the sediment and providing a working half and an archived half. The top (~50 cm) of each working half was sectioned vertically at 2-cm increments, creating "slices" for analysis; these "slices" (samples) were then freeze dried for 48 hr, removing all water.

Sediment bulk density

Determination of sediment bulk densities for each core was important in the calculation of mass accumulation rates, carbon sequestration rates, and carbon stocks. The gray-scale value of a CT scan is primarily related to a material's density, with lighter values more dense and darker values less dense (e.g., black indicates air). Thus, a relationship between CT-derived grey-scale value and a subset of experimentally determined dry bulk densities was derived. Sediment bulk density was experimentally determined every 2 cm for the top 50 cm of each reference site core using a method described by Howard et al. (2014). Briefly, known volumes of wet sediment (0.5 -1 cm^3) were sampled using syringes and placed on pre-weighed dishes. Each sample was weighed, dried at 60 °C for 24 hr, and reweighed at room temperature.

Radionuclides

We employed two age dating techniques using the radioisotopes ^{210}Pb and ^{137}Cs, which are commonly used in tidal wetland environments. ^{210}Pb is naturally produced in the environment in two ways. As part of the ^{238}U decay series, ^{226}Ra decays within sediments to ^{222}Rn, which is released to the atmosphere as a gas. ^{222}Rn then decays to ^{210}Pb and is deposited on land by atmospheric fallout. This form of ^{210}Pb is known as unsupported or excess ^{210}Pb, and often accumulates and decays in marine sediments following erosion from catchment topsoils. ^{210}Pb is also produced within sediment from the decay of ^{226}Ra. This ^{210}Pb decays to ^{214}Pb and is known as supported ^{210}Pb, because unlike excess ^{210}Pb it is constant with depth. Assuming a constant deposition rate and a relatively unmixed profile, the activity of excess ^{210}Pb can thus be calculated from the total ^{210}Pb profile and the supported ^{210}Pb profile determined by measurement of ^{214}Pb. The slope of the activity of excess ^{210}Pb with depth $\left(\frac{\lambda}{\mathbf{SAR}}\right)$ provides an estimate of sediment accumulation rate (Wheatcroft et al. 2013):

$$\mathbf{A_z} = \mathbf{A_0 e^{\left(\frac{-\lambda}{SAR}\right)z}}$$

where A_z and A_0 is the activity of excess ^{210}Pb at a given depth (z) and at 0 cm, respectively. λ is the ^{210}Pb decay constant (0.03101/yr) and SAR is the sediment accumulation rate (mm/yr).

^{137}Cs, primarily deposited as fallout from atmospheric nuclear weapons testing, offers an additional estimate of the sediment accumulation rate, assuming its deposition started when weapons testing

commenced in 1954, peaked in 1963, and fell sharply thereafter due to the end of aboveground nuclear weapons testing.

Samples were prepared for radionuclide measurement by first removing large pieces of plant material from the dried sediment, then grinding the sample to a homogeneous consistency using a mortar and pestle. Approximately 20 – 40 g of material were weighed into jars and the volume of the compacted and leveled sediment was recorded. Each sample was counted for ≥24 hr on Canberra gamma detectors and the activities of the radionuclides ^{210}Pb, ^{214}Pb, and ^{137}Cs were measured at their respective photopeaks (46.5, 352.0, and 661.6 keV) (Wheatcroft and Sommerfield 2005).

Mass accumulation rates (MAR; g/cm^2/yr) were calculated from the slope ($\overline{\frac{\lambda}{\mathbf{MAR}}}$) of excess ^{210}Pb activities plotted against cumulative mass (m; g/cm^2), determined using the change in depth and bulk density:

$$\mathbf{A_z = A_0 e^{\left(\frac{-\lambda}{MAR}\right)m}}.$$

Carbon content

Analyzed with sediment accumulation rates, sediment carbon densities (carbon concentrations) allow us to quantify carbon sequestration rates within the restoration site and nearby least-disturbed reference sites. Carbon densities also allow calculation of estimated carbon losses that occurred when the restoration site was diked and drained, and prediction of the post-restoration carbon sequestration capacity of the restoration site.

Loss on ignition (LOI) was used to measure organic matter content within the sediment samples, and a relationship between organic matter and organic carbon content was additionally determined for a subset of samples using an automated elemental analyzer (CHN analyzer). The LOI technique consisted of weighing the freeze-dried sediment before and after combustion in a muffle furnace at ~550 °C for 4-8 hr (Heiri et al. 2001). Sample preparation for CHN analysis consisted of packaging ~150 mg of dried sediment into a tin capsule, followed by instrumental analysis (Howard et al. 2014). Two samples, one with the highest measured organic content and one with the lowest, from each reference core were measured. To bolster these data, samples from two other northern Oregon estuaries (Youngs Bay and Salmon River) (Peck 2017) were included when determining the relationship between LOI and CHN.

Mean carbon density within the top 50 cm for each core was calculated by averaging the product of dry bulk density and the fraction of organic carbon for each 2-cm increment. Values of carbon density for the reference sites allowed us to calculate both the mass of carbon lost after diking in the restoration site and the mass of carbon that could potentially be stored after restoration.

Carbon sequestration rates (also called "carbon accumulation rates" or CARs, g C/m^2/yr) were calculated in a similar manner to mass accumulation rates; however, the cumulative mass of organic carbon (m_C; g C/cm^2), calculated as the cumulative mass multiplied by the percent organic carbon, was plotted against excess ^{210}Pb activity:

$$A_z = A_0 e^{\left(\frac{-\lambda}{CAR}\right)^m}.$$

To help interpret results, we calculated a rough approximation of the time period represented by the sediment accumulation, mass accumulation and carbon sequestration rates. To determine the approximate time period, we divided the core depth used for the sediment accumulation rate calculation (in mm) by the sediment accumulation rate (in mm/yr), and rounded to the nearest 10 years (because this approach is unlikely to resolve smaller time periods). Sediment accumulation rates determined using ^{137}Cs represent the 61 years prior to 2015 coring, by definition (since ^{137}Cs first appeared in 1954).

Data analyses

Cores were classified as low marsh, high marsh, scrub-shrub tidal swamp, and diked pasture (Table 7), and statistics were calculated for these groupings (except for scrub-shrub tidal swamp, which had only one representative). For the SFC monitoring program as a whole, Mean Higher High Water (MHHW) has been used as the division between low marsh and high marsh, based on regional studies (Brophy et al. 2011, Janousek and Folger 2014). The average elevation of local MHHW at the SFC site and reference sites was 2.4 m NAVD88 (Brown et al. 2016). Core BM.A064 was intermediate in elevation, at 6 cm below local MHHW of 2.31 m NAVD88. Its vegetation also showed intermediate marsh characteristics, co-dominated by Lyngbye's sedge (typical of low marsh in this area) and creeping bentgrass (typical of mid to high marsh). For purposes of this study, BM.A064 was included in the high marsh average.

For the reference sites, we calculated means for sediment accumulation rate, mass accumulation rate, carbon density, and carbon sequestration rate (Table 8), but we excluded from those means the very high accumulation and sequestration rates observed in the low marsh cores (BM.A063 and DSI-L.A047). As described in the SFC Effectiveness Monitoring Plan (Brophy and van de Wetering 2014), our monitoring (and carbon core locations) included both high marsh that corresponded to the likely pre-European-settlement conditions at the SFC site, and low marsh that corresponded to current elevations at the SFC site (due to subsidence). We used the mean calculated from the high marsh and scrub-shrub tidal swamp to understand of the likely functions of the SFC site before restoration, and its potential functions after restoration and equilibration to local sea level. We used the low marsh sediment accumulation rates to help interpret likely climate change/sea level rise resilience at the SFC site and other tidal wetlands in the Tillamook Bay estuary (see "**Discussion**" and "**Significance**" below).

Descriptive statistics were calculated for the carbon cores, representing variability within each core. A t-test was used to compare carbon densities and recent sediment accumulation, mass accumulation, and carbon sequestration rates (during the diked period) at the four SFC site cores, versus the three high marsh and scrub-shrub tidal swamp reference cores. However, due to the low number of replications in other groupings (n=2 for historical rates at SFC, n=2 for high marsh reference, n=2 for low marsh reference, n=1 for scrub-shrub tidal swamp), we were unable to make other statistical comparisons.

Results

CT scans

The CT scans showed that the sediment cores were in good condition following collection and transportation; many biogenic and sedimentary structures typical of marsh sediment were well preserved within the top 50 cm of each core (Figure 8). Many of the reference site cores had roots present (Figure 8 F-J). There was much less plant material within the restoration site cores, probably due to site drainage, soil tillage, and accompanying decomposition of subsurface plant material.

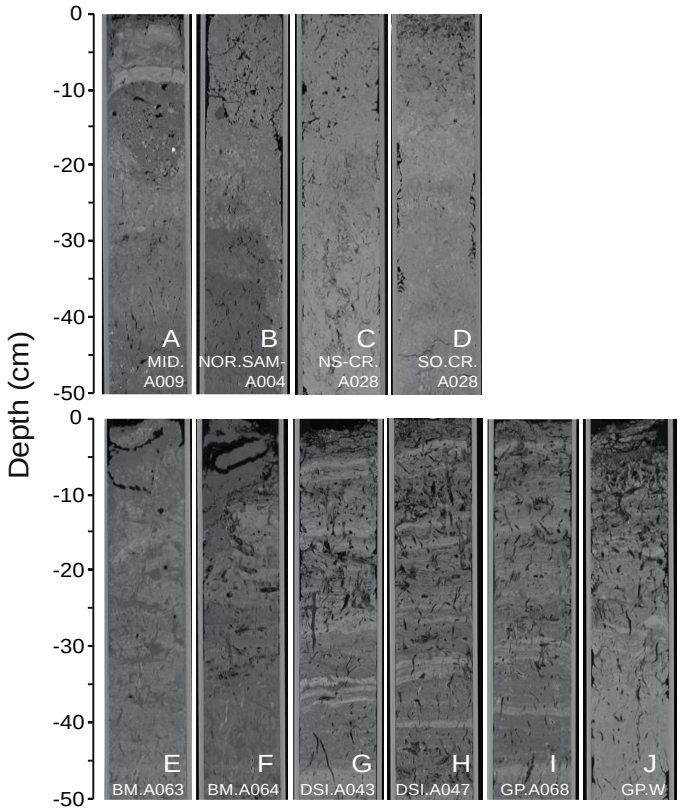

Figure 8. CT scans of the top 50 cm of each core. Lighter regions are more dense, while darker regions are less dense. Scans A – D are from cores collected in the restoration area. Scans E – J are from cores collected in the least-disturbed reference sites.

Sediment dry bulk density in reference site cores was strongly correlated with CT-derived grayscale value (Figure 9). This simple linear regression ($y = 0.012x - 0.62$, $R^2 = 0.70$) was used to calculate dry bulk density from the CT scans for the cores collected at the restoration site.

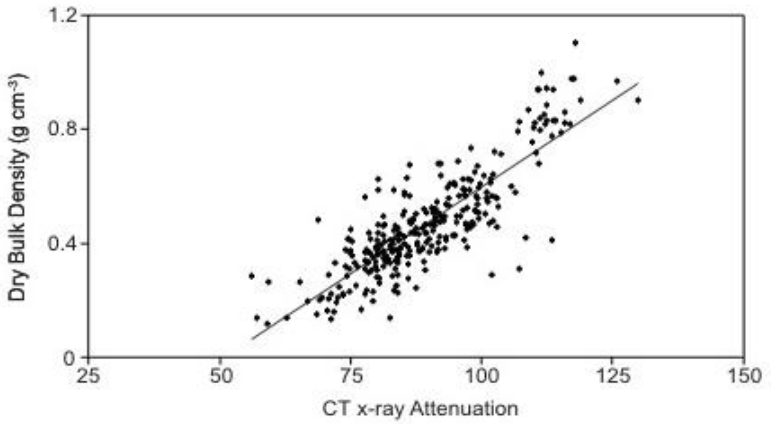

Figure 9. Relationship between dry bulk density measured directly from reference site cores and 8-bit (0 – 255) grayscale values of CT x-ray attenuation (n = 302). The linear regression has an R^2 value of 0.70, a slope of 0.012, and a y-intercept of -0.62.

Radioisotope profiles

Graphs ("profiles") of excess ^{210}Pb by depth (e.g. Figures 10 and 11) are used to determine whether the ^{210}Pb method is working as expected, and to reveal outliers or other problematic data points that should be omitted when estimating sediment accumulation and carbon sequestration rates. When the method is working well and surface sediments are not heavily disturbed by biologic activity, excess ^{210}Pb should show a steady decrease with increasing depth. This study's profiles of excess ^{210}Pb generally showed this pattern (Figures 10 and 11), but there were some individual data points (core slices) that did not follow this pattern (gray points in Figures 10 and 11); these points were excluded from the calculation of sediment accumulation rate. For instance, any sediment slices with error ranging below the detection limit of the γ-ray spectrometers (3 Bq/kg) were excluded. In some cases, surface sediment organic content can dilute the inorganic component of the slice, causing low ^{210}Pb activities. The surface slice for GP.A068 showed this effect, and was therefore omitted. Multiple profiles exhibited outliers, which could be due either to a change in sediment grain size or soil being moved from one depth to another by burrowing organisms; these outliers were also excluded from the regression (e.g., lowest slice for NS-CR.A073).

At two of the restoration site cores (MID.A009, NOR-SAM.A004), the ^{210}Pb profile had two different sections corresponding to recent versus older (historical) time periods. For NOR-SAM.A004, the slope differed between the two sections, suggesting the rate of sediment accumulation (and associated carbon sequestration) has changed during recent years. The upper, recent section of the profile had a steeper slope, representing a faster accretion rate in the past few decades, while the lower, historical section showed a slower accretion rate.

In contrast to the expected ^{210}Pb profile, when the ^{137}Cs method is working well, ^{137}Cs profiles should show a "mountain-shaped" curve belowground, with a peak corresponding to the 1963 Partial Test Ban Treaty and a decrease in ^{137}Cs concentration from that point to the present. This pattern was not evident for most of the cores in this project. The ^{137}Cs profiles for all but two cores showed higher-than-expected concentrations of ^{137}Cs that peaked at or near the sediment surface (data not shown), suggesting upward movement and loss of ^{137}Cs after deposition. Unlike ^{210}Pb, ^{137}Cs is relatively mobile, becoming un-adsorbed from sediment particles after deposition due to changes in sediment chemistry

such as salt intrusion, which allows this "post-depositional remobilization." Cores with profiles indicating post-depositional remobilization cannot be used for the ^{137}Cs method. However, rapid accumulation of sediment can prevent post-depositional remobilization by reducing the time during which remobilization can occur.

Of all the study cores, only two cores showed the expected sub-surface peak in ^{137}Cs concentration, and these were the cores with the fastest sediment accumulation rates (BM.A063 and DSI-L.A047) (Figure 12). Two dates could be derived from the BM.A063 ^{137}Cs profile: the initial appearance within the core and the peak. Thus, the average of the dates was used to calculate the sediment accumulation rate. Because there was still ^{137}Cs at the surface of DSI-L.A047, only a minimum accretion rate could be determined; the actual rate may have been considerably higher.

Sediment and mass accumulation

The mean rates of recent and historical sediment accumulation for the SFC site were 4.1 and 1.3 mm/yr, respectively (Table 8). Within this mean, recent rates of sediment accumulation at the SFC site varied widely among cores, ranging from 1.2 to 6.0 mm/yr; these rates represented the past 30-60 yr, while the historical rates represented earlier time periods up to 140 yr ago (Table 8).

Among the high marsh and scrub-shrub tidal swamp reference site cores, mean sediment accretion was 2.2 mm/yr and represented the past 90-150 yr (Table 8). Sediment accretion rates were not significantly different among the reference cores (Grubb's test for statistical outliers, $P < 0.05$), nor was this mean significantly different from the mean recent sediment accumulation rate at the SFC site (Student's t-test, two-tailed, $P = 0.18$). By contrast, the low marsh cores BM.A063 and DSI-L.A047 were accreting much faster, at 10 and >18 mm/yr, respectively, during the past 60 years (Table 8).

Mass accumulation rates (quantity of sediment deposited) better account for sediment compaction than sediment accumulation rates, since density changes with depth are accounted for in the calculation. Because of this, mass accumulation rates are often preferred measures of accumulation. The mean recent and historical mass accumulation rates for the restoration site were 2.2 and 0.61 kg/m^2/yr, respectively (Table 8). The mass accumulation rate measured in the least-disturbed reference sites was 0.97 kg/m^2/yr, which was not significantly different from the recent rate at the SFC site (Student's t-test, two-tailed, $P = 0.13$).

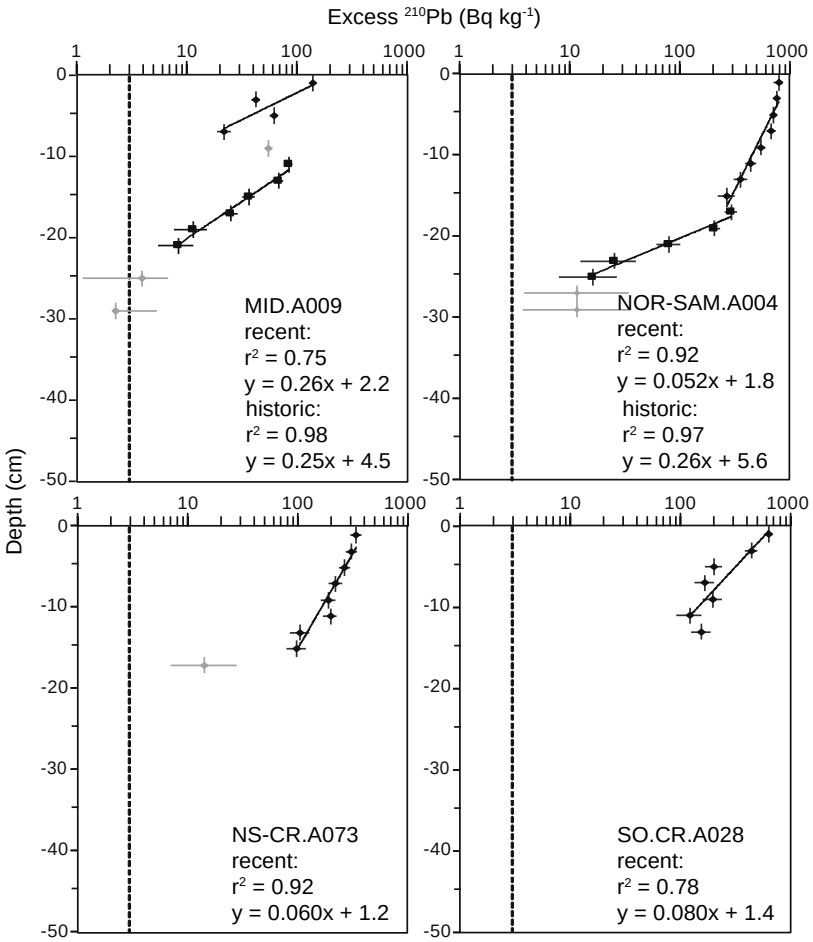

Figure 10. Depth profiles of excess ^{210}Pb measured in each restoration site core. The vertical dashed line indicates the detection limit (3 Bq/kg) of the gamma detectors. The vertical bars indicate the height of the "slice" of sediment sampled (2 cm) and the horizontal error bars represent the detector error. The gray points were not included in the regression. The top two profiles exhibited a change in accretion rate; the upper sections (black diamonds) were used to calculate recent sediment accumulation rates and the lower sections (black squares) were used to calculate historical sediment accumulation rates. The lower two graphs represent recent accumulation rates only.

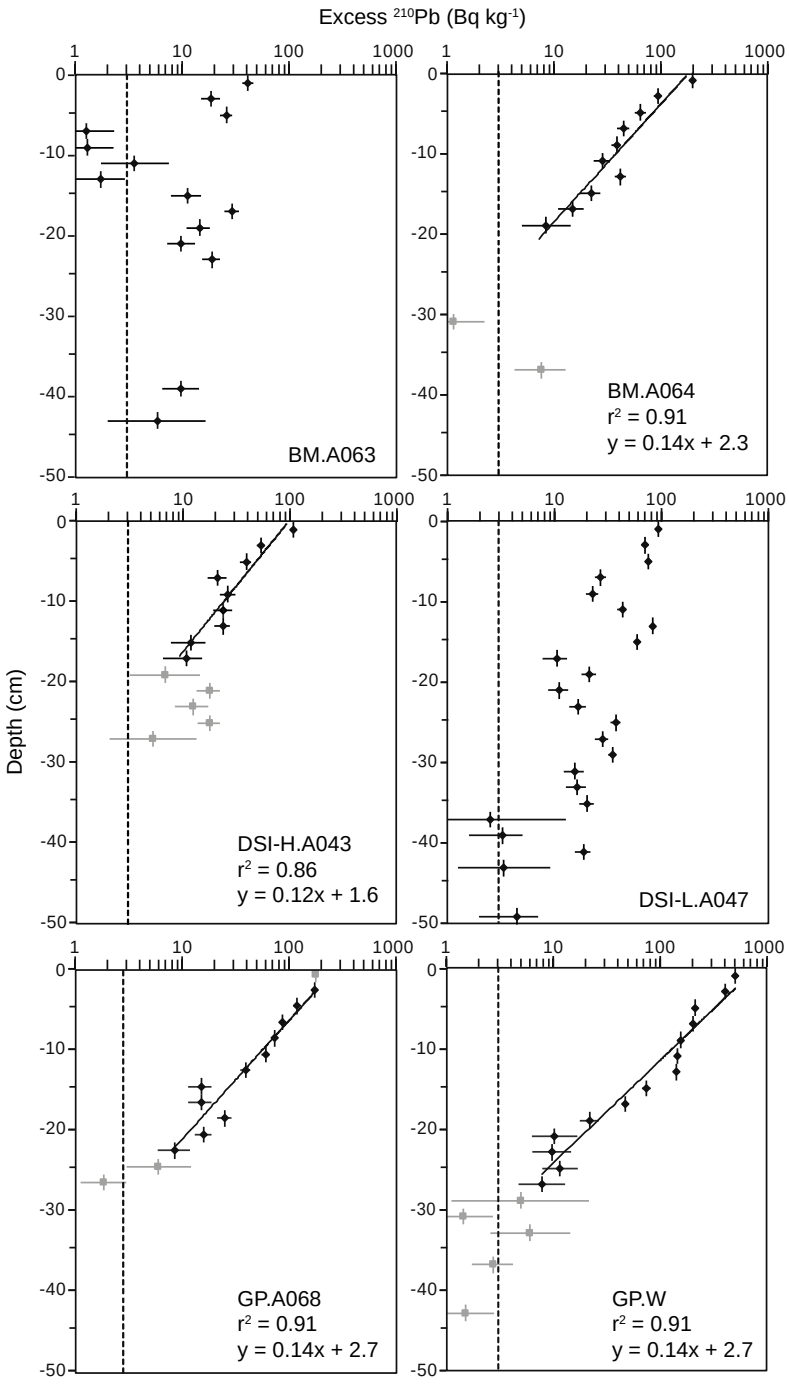

Figure 11. Depth profiles of excess ^{210}Pb activities measured in each reference site core. The vertical dashed line indicates the detection limit (3 Bq/kg) of the gamma detectors. The vertical bars indicate the height of the "slice" of sediment sampled (2 cm) and the horizontal error bars represent the detector error. The gray points were not included in the regression. The black points were used to calculate sediment accumulation rates.

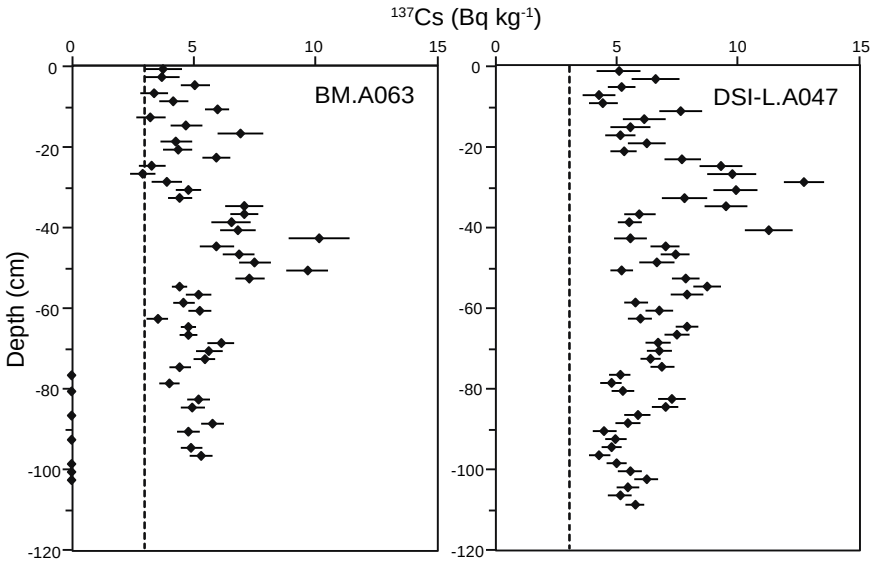

Figure 12. ^{137}Cs concentration measured in BM.A063 and DSI-L.A047. The vertical dashed line indicates the detection limit (3 Bq/kg) of the gamma detectors. The horizontal error bars represent the detector error; the height of each "slice" is the same as in the previous figure (2 cm).

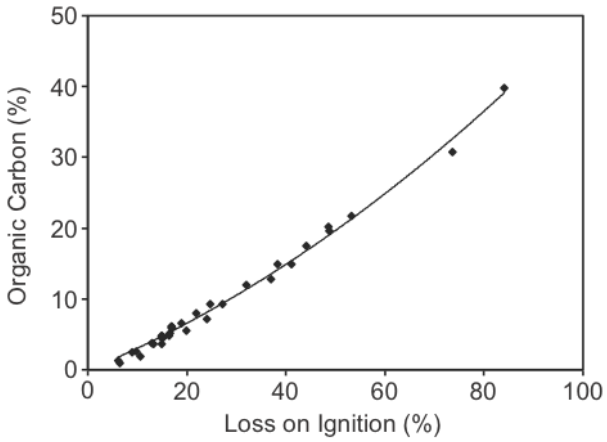

Figure 13. Relationship between organic carbon (C_{org}), measured using elemental (CHN) analysis and LOI, using data from this study and from other Northern Oregon sites in the Salmon River and Youngs Bay estuaries (n = 34) (Brophy et al. 2017, Peck 2017). The R^2 value of the regression is 0.99 and the equation is $C_{org} = 0.0021 \bullet LOI^2 + 0.29 \bullet LOI$.

Relationship between soil organic matter and carbon content

The relationship between LOI-derived organic matter and organic carbon measured by elemental analysis (Figure 13) agreed well with equations calculated by others (Morris and Whiting 1986; Craft et al. 1991). Crooks et al. (2014), however, determined quite a different relationship for the Snohomish estuary (Washington), indicating the importance of determining region-specific relationships. Given the closeness of fit, the relationship calculated here was deemed appropriate for northern Oregon tidal wetlands and was thus applied to all core samples to convert organic matter to organic carbon. The relationship is quadratic because sediments high in organic matter are more subject to decomposition

(Craft et al. 1991). Sediments that are enriched in OM are subject to greater breakdown by soil organisms, a process which requires macronutrients such as N. Thus, as OM becomes enriched in compounds high in organic carbon (e.g., refractory organic compounds, fatty acids, and methane) through decomposition, the ratio of C_{org}:OM increases while the ratio of N: C_{org} decreases (Peck 2017).

Carbon profiles, carbon densities and sequestration rates

Profiles of organic carbon showed a general decrease with depth (Figure 14) due to decomposition during burial. In general, restoration site cores (Figure 14A) had carbon densities similar to the reference sites (Figure 14B). However, one core stood out: core GP.W, in a scrub-shrub tidal swamp, had much higher C_{org} content than cores at the SFC site or the high or low marsh reference sites, particularly in the top 20 cm (Figure 14B).

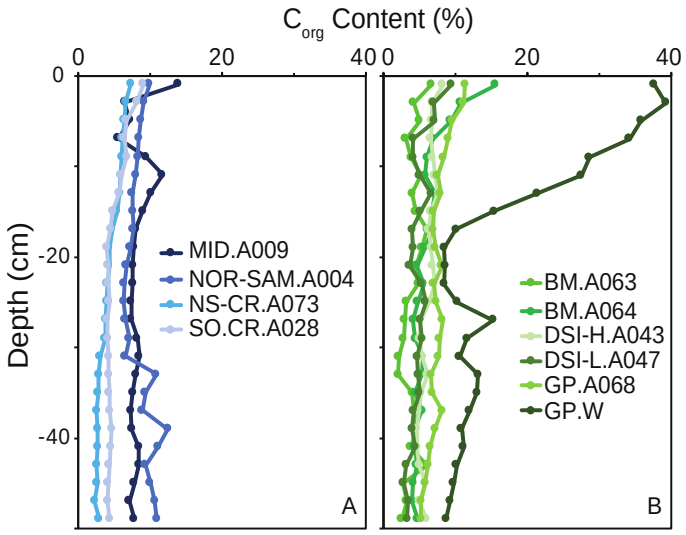

Figure 14. Organic carbon profiles for each core. Subplot A shows cores at the restoration site and subplot B shows cores at the reference sites.

Mean sediment carbon densities for the restoration and reference sites were not significantly different, averaging 0.034 and 0.031 g C_{org}/cm^3, respectively (Table 8) (Student's t-test, P = 0.91). However, carbon sequestration rates within the restoration site differed between recent and historical periods, averaging 150 and 51 g $C_{org}/m^2/yr$ for recent and historical accretion, respectively (Table 8) – primarily driven by the much higher sediment accumulation rates described above. The mean carbon sequestration rate within the reference sites (85 g $C_{org}/m^2/yr$, Table 8), was not significantly different from the mean recent rate at the SFC site (150 g $C_{org}/m^2/yr$, Table 8) (Student's t-test, two-tailed, P = 0.18).

Table 8. Sediment accumulation rates, mass accumulation rates, mean carbon densities within the top 50 cm of sediment, and carbon sequestration rates for each carbon core location. Mean rates (±1 SE) are provided for both the restoration and reference sites. Rates measured at low marsh cores (BM.A063 and DSI-L.A047) were not included in the overall reference means below; see "**Methods**" above.

Site	Core Location		Sediment accumulation rate (mm/yr)	Mass accumulation rate (kg/m²/yr)	Mean soil carbon density (g C_{org} /cm³)	Carbon sequestration rate (g C_{org}/m²/yr)	Approx. time period represented (yr)*
SFC (restoration)	MID.A009	recent	1.2 ± 0.5	0.66 ± 0.26	0.038 ± 0.005	44 ± 19	0-60
		historical	1.3 ± 0.1	0.61 ± 0.04		51 ± 4	60-140
	NOR-SAM.A004	recent	6.0 ± 0.7	2.3 ± 0.3	0.031 ± 0.004	190 ± 20	0-30
		historical	1.2 ± 0.1	0.51 ± 0.05		35 ± 4	30-100
	NS-CR.A073	recent	5.2 ± 0.6	3.5 ± 0.4	0.032 ± 0.007	220 ± 30	30
		historical	-	-		-	
	SO.CR.A028	recent	3.9 ± 1.0	2.5 ± 0.7	0.035 ± 0.004	160 ± 40	36
		historical	-	-		-	
	MEAN (recent)		**4.1 ± 2.1**	**2.2 ± 1.2**	**0.034 ± 0.003**	**150 ± 77**	
	MEAN (historical)		**1.3 ± 0.1**	**0.61 ± 0.07**		**51 ± 11**	
Reference	BM.A063 (low marsh)		10.0 ± 3	6.4 ± 1.7	0.025 ± 0.004	260 ± 70	60
	BM.A064 (high marsh)		2.2 ± 0.2	1.0 ± 0.1	0.028 ± 0.005	69 ± 8	90
	DSI-H.A043 (high marsh)		2.6 ± 0.4	1.3 ± 1.2	0.031 ± 0.005	90 ± 13	90
	DSI-L.A047 (low marsh)		>18	>7.9	0.023 ± 0.006	>420	60
	GP.A068 (high marsh)		2.2 ± 0.3	0.95 ± 0.01	0.033 ± 0.005	72 ± 7	110
	GP.W (scrub-shrub tidal swamp)		1.8 ± 0.1	0.63 ± 0.04	0.046 ± 0.024	110 ± 10	150
	MEAN (excluding low marsh)		**2.2 ± 0.3**	**0.97 ± 0.27**	**0.031 ± 0.008**	**85 ± 19**	

* Rounded to the nearest 10 yr. Approximate time periods are shown as a range of years before 2015 (e.g., 60-140 represents approximately the late 1800s through the 1950s).

Soil carbon stocks

The soil carbon stocks for each core location were calculated as the product of carbon density and sediment depth (Kauffman and Donato 2012; Table 9). The CT scans showed little lithology change with depth in the restoration site cores and for reference site cores BM.A063, DSI-L.A047, and GP.A068, so the full core depths were used to calculate soil carbon stocks at these locations. However, the CT scans showed abrupt changes in lithology (from coarse sandy material below, to finer grained material above) within BM.A064, DSI-H.A043, and GP.W, so only the depths above the lithology changes were considered at these locations. Carbon density was only available for the top 50 cm of each core (for which slices were analyzed for LOI), and the average density for the top 50 cm was assumed to be representative of the full depth for which no lithology change was observed. The CO_2 equivalent pool for

each core was calculated using a conversion factor of 3.67 (the ratio of the molecular weight of CO_2 to the atomic weight of carbon) (Table 9).

Table 9. Depth of each core used to calculate soil carbon stock, and resulting carbon stocks and CO_2 equivalents for each location.

Site type	Core location	Core depth used to calculate carbon stock (cm)*	Soil organic carbon stock (t/ha)	CO_2 equivalent pool (t/ha)
Restoration (SFC)	MID.A009	115.5	484	1776
	NOR-SAM.A004	99.5	335	1231
	NS-CR.A073	83.0	295	1083
	SO.CR.A028	78.5	302	1109
Reference	BM.A063	120.0	330	1211
	BM.A064	82.0	253	927
	DSI-H.A043	116.0	396	1452
	DSI-L.A047	110.5	280	1026
	GP.A068	262.5	953	3497
	GP.W	170.0	860	3157

* Core depth shows the depth used for the carbon stock calculation. For example, a depth of 262.5 cm was used for core GP.A068 because no lithology change was observed to that depth.

Impacts of diking and restoration on blue carbon

Using information collected at a suitable reference site, we can estimate the mass of soil carbon lost when the restoration site was diked and the mass of carbon that will be stored in soil following restoration of the SFC site. These masses are calculated as the same value, since the SFC restoration site has not subsided below the typical lower elevation boundary for vegetated marsh, around mean tide level (around 1.5 m NAVD88 at SFC). (If it had subsided below that boundary, the rate and ultimate total C storage would be reduced, since non-vegetated wetlands accumulate less sediment and carbon [Crooks et al. 2014]). The high marsh at Dry Stocking Island core DSI-H.A043 is a suitable reference for this analysis, since it is the predominant historical wetland type at SFC, and the likely future wetland type for the SFC site once it equilibrates with sea level.

To determine the carbon lost after diking, the volume of soil that would ultimately fill the restoration site was calculated for each zone; this is equal to the volume that was lost via subsidence. The summed total for all zones allowed us to predict carbon masses lost, and potentially gained in the future, for the entire SFC restoration project. The areas and current elevations of each zone are summarized in Table 10. Additional carbon in the form of aboveground biomass was lost at the time of agricultural conversion due to vegetation removal, particularly for those portions of the SFC site that were historically scrub-shrub and forested tidal swamp (Ewald and Brophy 2012), but estimation of those losses was beyond the scope of this project.

Based on DSI-H.A043 (which was typical of high marsh at Dry Stocking Island), the reference site high marsh elevation is 2.61 m NAVD88 (Table 7). Historical vegetation mapping (Hawes et al. 2008) shows that the majority of the SFC site was occupied by high marsh and shrub/forested tidal swamp before diking. Historically, within the SFC site, high marsh and shrub/forested tidal swamp were probably found at similar elevations, with spatial distribution controlled by salinity (Brophy 2009, Brophy et al. 2011).

Therefore, with long-term accretion, we expect the SFC site to attain an elevation similar to the reference site high marsh (i.e. 2.61 m NAVD88). The expected long-term elevation increase at the SFC site is thus between 0.24 and 0.75 m (depending on the zone), and the added sediment volume per zone will be between 20,000 and 380,000 m^3 (Table 10). Using the mean carbon density for the top 50 cm of DSI-H.A043, which is 0.031 g C_{org}/cm^3 (Table 8), the masses of organic carbon lost range from 680 to 13,000 t C_{org} and the total mass is 27,000 t C_{org} (Table 10). Assuming a total area of 139 ha, this mass translates to a total of 200 t C/ha that was released to the atmosphere following diking. Applying a conversion factor of 3.67 to calculate the mass of CO_2 equivalent (Kauffman and Donato 2012), about 100,000 t CO_2 or 720 t CO_2/ha have been released since diking (Table 10). These values also represent the CO_2 equivalent of carbon that could be stored following restoration. This quantity of potential carbon storage (27,000 t C_{org}) is equivalent to the greenhouse gas emissions from about 21,000 passenger cars being driven for a year at average vehicle mileage (US EPA 2018). The time required to achieve this level of carbon storage will be the time required to achieve the vertical accretion described above, i.e., 0.23 to 0.71 m of accretion (depending on the zone). This time is difficult to estimate, as it will depend on the rate of sea level rise, available sediment supply, frequency of flooding, and other controlling factors in the complex hydrodynamic environment of Tillamook Bay.

Our estimate of the mass of carbon lost from the SFC site (200 t C_{org}/ha) – and thus the potential mass of carbon stored in the future (also 200 t C_{org}/ha) -- was slightly lower (on a per-hectare basis) than the estimate generated by Crooks et al. (2014) in the Snohomish estuary (240 tons/ha). Three factors could cause this difference: 1) soil carbon density; 2) the elevation used to estimate historical marsh surface elevation and likely future wetland surface elevation; and 3) the degree of subsidence at the restoration sites. Carbon density was higher in our reference core (0.031 g C_{org}/cm^3) compared to the carbon density used for the calculation in Crooks et al. (2014) (0.025 g cm^3), which on its own, would result in higher past carbon loss and potential future storage. The reference site elevation for our study (2.61 m NAVD88) was slightly lower than the value used at the Snohomish estuary (2.76 m NAVD88, Crooks et al. 2014); this would slightly reduce carbon loss and future carbon storage. The largest factor was clearly the lesser degree of subsidence at the SFC site. Subsidence ranged from 0.24 to 0.75 m at the SFC site (Table 7), compared to 0.7 to 1.7 m at the Snohomish sites (Crooks et al. 2014). Less subsidence at the SFC site means less past carbon loss (because oxidation of soil organic matter is a major cause of subsidence); and less potential future carbon storage. However, the lesser degree of subsidence at the SFC site indicates a higher likelihood of wetland resilience under sea level rise scenarios, and resilient wetlands are more likely to continue providing carbon sequestration services into the future.

Table 10. Approximate masses of carbon and CO_2 lost, and likely future carbon and CO_2 equivalent storage, for SFC zones. Masses were normalized to area for each zone within the SFC restoration project and totaled across zones. The expected elevation for the SFC site after equilibration with sea level, and the expected carbon density for the SFC site, were both assumed to be similar to the DSI-H.A043 core location (2.61 m NAVD88 and 0.031 g C_{org}/cm^3, respectively). Calculated values are rounded to 2 significant digits.

Parameter	North Zone	Middle Zone	South Zone no crop	South Zone crop	Nolan crop	Nolan grazed	Nolan ungrazed	Total
Area (ha)	17	60	6	34	9	9	6	139
Elevation (m)	2.31	1.97	1.95	1.90	2.20	2.38	2.11	
Change in elevation (m)	0.30	0.64	0.66	0.71	0.41	0.23	0.50	
Change in volume (m^3)	50,000	380,000	39,000	240,000	36,000	20,000	28,000	800,000
Total mass of carbon (t C)	1,700	13,000	1,300	8,300	1,200	680	940	27,000
Carbon storage (t C/ha)*	100	220	230	240	140	80	170	200
CO_2 equivalent total mass (t CO_2)*	6,300	48,000	4,900	30,000	4,500	2,500	3,500	100,000
CO_2 equivalent storage (t CO_2/ha)*	380	800	830	890	510	290	630	720

* Potential future carbon storage is considered equal to estimated past losses of carbon due to diking; see text for details.

Discussion

Climate change resilience

In this carbon core study, the mean sediment accumulation rate for reference sites (2.2 mm/yr) exceeded the estimated sea level rise rate within Tillamook Bay of approximately 1.0 mm/yr over the past century (Komar et al. 2011). A similar result was observed by Thom (1992) in the Salmon River estuary; the two cores analyzed showed accretion rates of 3.0 mm/yr under a relative sea level rise of 1.7 mm/yr. Our past studies have shown that least-disturbed high marsh and tidal swamp in Oregon are found at elevations slightly higher than MHHW (Brophy 2009, Brophy et al. 2011), and this was true of this study's high marsh and scrub-shrub sites (Table 7); this may help explain why sediment accretion slightly exceeds sea level rise.

It is not surprising that high marsh and tidal swamp accretion rates would equal or exceed local sea level rise rates, because mature tidal wetlands tend to exist in equilibrium with sea level (Morris et al. 2002). As sea level rises, multiple feedbacks between morphology and vegetation allow the wetland surface to accrete at a similar pace. As tidal inundation increases, more suspended sediment can settle onto the wetland surface. Wetland vegetation assists the process by trapping more sediment, reducing wave energy, and increasing organic matter accumulation both above and below the wetland surface (Kirwan and Megonigal 2013). Our carbon core results suggest that these processes are intact, and the locations sampled have kept pace with past sea level rise.

The two low marsh reference cores, BM.A063 and DSI-L.A047, showed very high accretion rates. These cores sampled the lowest-elevation wetlands among all the reference sites (0.25 m and 0.44 m below local MHHW, respectively), and their rapid accretion was probably due to their low elevation. As wetlands transition from low to high marsh or tidal swamp, they often accrete much faster than areas already high in elevation (Morris et al. 2002, Chmura et al. 2003). This is probably especially true for low marsh in areas of rapid marsh advance, which is the case in Tillamook Bay (Dicken 1961, Komar et al. 2004). Kirwan et al. (2016) noted that vertical accretion within lower-elevation tidal marsh may be the best indication of marsh resistance to drowning under accelerating sea level rise. This is because high marshes vertically accrete to a high elevation within the tidal frame, thereby reducing frequent flooding, but low marshes are frequently inundated, simulating the stress of higher sea level. If these areas continue accreting under such stress, the wetland may avoid future drowning.

Accretion rates relative to past sea level rise are only part of the picture needed to understand climate change resilience at tidal wetlands. Equally important, tidal wetlands must have a strong sediment supply to withstand future accelerated sea level rise (Kirwan et al. 2010). The Tillamook watershed has an abundant sediment supply (Komar et al. 2004), which bodes well for the estuary's climate change resilience. Peck (2017) estimated that about 21,000 tons of sediment are deposited on tidal wetlands in the Tillamook Bay estuary each year; and she estimated the total sediment load for the estuary at 160,000 tons/yr. Therefore, most sediment is exported from the bay to the continental shelf each year, indicating the estuary is probably not sediment-limited (Peck 2017).

A recent regional study (Thorne et al. 2018) was less optimistic regarding the resilience of Pacific Northwest tidal marshes under higher sea level rise scenarios. The authors found that "tidal wetlands are highly vulnerable to end-of-century submergence, with resulting extensive loss of habitat." Clearly, the topic is still open to discussion, and we recommend continued research to help resolve this important question.

Carbon densities, carbon stocks, carbon sequestration rates, and wetland elevation

Mean soil carbon densities were similar between the least-disturbed high marsh/shrub reference cores (0.031 g C_{org}/cm^3) and restoration cores (0.034 g C_{org}/cm^3) (Table 8). These carbon densities were roughly similar to the global mean carbon density of 0.039 g/cm^3 for tidal saline wetlands published by Chmura et al. (2003). Comparisons to other Pacific Northwest tidal wetlands are more useful, but data are very sparse (Cornu 2017). Carbon densities in this study were somewhat higher than those reported by Crooks et al. 2014 for restored and natural sites in the Snohomish estuary, Washington; in Crooks et al., the average of reported soil carbon densities was 0.024 g C_{org}/cm^3 for 5 restored sites and 0.028 g C_{org}/cm^3 for 3 least-disturbed reference sites. The mean carbon density at the SFC site was slightly higher than at the Wallooskee-Youngs restoration site, Youngs Bay estuary, Oregon (part of the lower Columbia River estuary) (0.023 g C_{org}/cm^3, Brophy et al. 2017); the average carbon density in high marsh and scrub-shrub tidal swamp reference sites in the current study was very similar to that measured in high marsh/shrub swamp in the Youngs Bay estuary (0.030 g C_{org}/cm^3, Brophy et al. 2017).

The scrub-shrub wetland at Goose Point (core GP.W) had the highest carbon density observed in this study (0.046 g C_{org}/cm^3, Table 8), with densities particularly high in the top 20 cm (Figure 14). This led to a very high soil carbon stock in this scrub-shrub tidal swamp – higher than any other location in this study except the nearby high marsh at Goose Point (core GP.A068) (Table 9). Data on soil carbon in Pacific Northwest scrub-shrub tidal swamps are extremely sparse (Cornu 2017), but two other studies in

Oregon (Brophy 2009, Brophy et al. 2011) found that least-disturbed scrub-shrub tidal wetlands had the highest surface soil organic matter contents of all three major tidal wetland habitat classes (emergent, scrub-shrub, and forested). These observations hint at the unique characteristics of this understudied wetland type, and its potential importance as a provider of carbon sequestration services.

Carbon sequestration rates were closely tied to elevation. The low marsh cores BM.A063 and DSI-L.A047 showed very high carbon sequestration rates of 260 and >420 g $C_{org}/m^2/yr$, respectively (Table 8) – about 5 and 8 times higher than the other reference locations. These rates were considerably higher than the global rate of 91 g $C_{org}/m^2/yr$ (IPCC 2014), and similar to rates reported for rapidly-accreting restoration sites in the Snohomish estuary, Washington (Crooks et al. 2014) and for low marsh in the Youngs Bay estuary, Oregon (Brophy et al. 2017). Carbon sequestration rates within the high marsh and scrub-shrub tidal swamp reference sites were lower (69 - 110 g $C_{org}/m^2/yr$, Table 8); this was expected, because these wetlands are located at a high elevation relative to the local tidal range. Similar sequestration rates (54 - 130 g $C_{org}/m^2/yr$) were observed in high marsh and scrub-shrub tidal swamp in the Youngs Bay estuary (Brophy et al. 2017). Carbon sequestration rates are primarily driven by sediment accretion rates (Chmura et al. 2003), and sediment accretion is generally higher in low marsh (due to more frequent inundation) and lower in high marsh (Morris et al. 2002). As sea level rise accelerates, carbon sequestration rates are likely to increase within former high marsh due to more frequent inundation and the associated increase in accretion -- provided accretion rates are sufficiently to prevent "drowning" (i.e. loss of vegetation due to excessive inundation).

Interestingly, the mean recent rate of carbon sequestration within the restoration site was quite high at 150 g $C_{org}/m^2/yr$, similar to the global mean rate (IPCC 2014) – and this was measured in 2015, prior to dike removal. Again, carbon sequestration rates are primarily driven by sediment accumulation rates; and as described above, sediment accumulation rates were high within the restoration site prior to dike removal. As shown by the feldspar marker horizon plot results, sediment is accumulating even faster after dike removal – and therefore carbon is probably also accumulating faster after restoration.

Despite relatively high sediment accumulation and carbon sequestration rates while diked, it is clear that diking of the SFC site led to large losses of carbon to the atmosphere, simply because the site has subsided substantially compared to the high marsh reference site. Subsidence of this type is commonly observed in diked tidal wetlands; it is caused by drainage of soils resulting in loss of soil organic matter through decomposition; by compaction of soils by farm machinery and livestock trampling; and by other factors (Frenkel and Morlan 1990, 1991). The SFC site's elevation loss indicates that despite its relatively high sediment accretion rate during recent years, sediment accretion has not compensated for subsidence, with elevation loss being the net result. As the SFC site equilibrates with sea level after restoration, it is expected to return to accumulating carbon at rates similar to nearby reference sites at similar elevations. This is expected to lead to accumulation of the same amount of carbon that was lost after diking – and potentially more, as the site equilibrates to rising sea level. However, very rapidly rising sea level could potentially "drown" the wetlands at the site if inundation is frequent and deep enough to prevent growth of sediment-trapping vegetation, preventing full restoration of the original carbon stocks.

Recent and historical accretion rates at SFC and reference sites

Historically (before diking), the SFC restoration site was a tidal wetland, with habitat types ranging from high marsh to Sitka spruce tidal swamp (Hawes et al. 2008). The historical high marsh at the site was

presumably similar to the Goose Point and Dry Stocking Island high marsh reference sites, which were selected as reference sites for this reason (Brophy and van de Wetering 2014). Therefore, the comparison between sediment accumulation, mass accumulation, and carbon sequestration rates at the SFC site versus the corresponding rates at the high marsh reference sites is of interest. We expected sediment accumulation rates to be similar between the historical (pre-diking) SFC restoration site and the high marsh and tidal swamp reference sites; lower after diking (due to loss of daily tidal inundation); and higher after dike removal and restoration (due to return of daily tidal inundation). However, we are also aware that even prior to restoration, winter floods regularly overtopped the dikes (Philip Williams and Associates 2002, NHC and HBH Consulting Engineers 2010, Levesque 2013), probably carrying large quantities of fluvial and marine-sourced sediment onto the site. In fact, 2014 sediment accretion monitoring using feldspar marker horizon plots showed that accretion was significantly higher in the still-diked SFC site compared to the reference sites, suggesting considerable sediment inputs from such floods (see "**Sediment accretion (feldspar marker horizon plots)**" above).

The carbon core data showed that sediment accumulation, mass accumulation, and carbon sequestration rates were similar (Student's t-test, $p > 0.10$) between the high marsh/scrub-shrub tidal wetland reference sites (2.2 mm/yr), and the recent period at the SFC site (4.1 mm/yr during the past 30-60 yr). Historical sediment accumulation rates, observed in only two cores at the SFC site, were lower: 1.3 mm/yr during the preceding period (from 30-140 or 60-140 years ago), compared to 2.2 mm/yr at the high marsh/scrub-shrub tidal wetland reference sites (representing the past 60-110 years). As mentioned above, the relatively high recent accumulation rates at the SFC site may be due to dike-overtopping flood events, combined with the subsided elevations at the site. After dike removal, we observed evidence of the quantities of sediment that could potentially be moved onto the site: coarse (sandy) flood deposits were observed extending nearly 100 m south from the Wilson River banks in the area north of NOR-SAM.A004 after winter 2016-2017.

The high sequestration rates during the recent period at SFC occurred prior to restoration, since the carbon cores were collected in 2015. Based on the post-restoration increase in sediment accretion rates observed using the feldspar marker horizon method (see "**Sediment accretion (feldspar marker horizon plots)**" above), C sequestration probably increased after restoration at the SFC site, since sequestration is generally driven by sediment accumulation rates (see "**Carbon densities, carbon sequestration rates, and wetland elevation**" above).

The relatively low historical sediment accumulation, mass accumulation and carbon sequestration rates measured in cores taken from the SFC site may be due to compaction of deeper sediments during the period of active agricultural use. Subsidence and compaction of surface and subsurface soils at diked tidal wetlands is a common phenomenon, first described in Oregon by Frenkel and Morlan (1991). It is caused by loss of organic matter from soil due to drainage and organic matter decomposition, plus compaction from machinery operations and livestock trampling – causes which were first identified in studies of European drainage projects (Williams 1970; Hutchinson 1980; Darby 1983). Tillage of the top layer of soil may decompact surface layers but fail to decompact deeper layers. However, the distinctly different historical and recent accumulation rates were observed only in the cores from the Middle and North zones of the SFC site, which have not been in active agricultural use for several years. By contrast, the South zone, which was actively tilled in recent years, did not show a distinct historical versus recent profile. Further analyses, such as additional sampling at the SFC site and other nearby agricultural fields, could help determine the prevalence and potential causes of these interesting results.

The other sediment accretion monitoring method included in this report – feldspar marker horizons – also showed rapid sediment accumulation within the restoration site and generally lower rates of sediment accumulation within the least-disturbed reference sites; and the general relationships between elevation and accretion rates were similar to the ^{210}Pb and ^{137}Cs methods, although absolute values differed. In general, the feldspar marker horizon method showed higher accretion rates, as would be expected (see next section).

Comparison of accretion rates from feldspar and carbon core methods

Annual accretion rates are expected to be higher for the feldspar marker horizon method compared to the carbon core method, because the feldspar method does not account for compaction of accumulated sediment over time (Cahoon et al. 2000). We compared pre-restoration data for locations where both types of data were obtained, and found that the feldspar method showed similar or higher accretion rates for most locations (Figure 15). For the low marsh on Dry Stocking Island (DSI-L.A047), the feldspar rate was aberrantly low compared to the carbon core rate. According to the landowner, this may have been due to foot traffic in the feldspar plots, which would have greatly compacted the deposited material. On the other hand, the feldspar rate was aberrantly high compared to the carbon core rate at site A04 in the North Zone at the SFC site; this may represent a single flood event that strongly affected this location during winter 2013-2014. Since the feldspar plots represent only the past few years, they are much more strongly influenced by recent depositional events, compared to the longer-term record of the carbon cores.

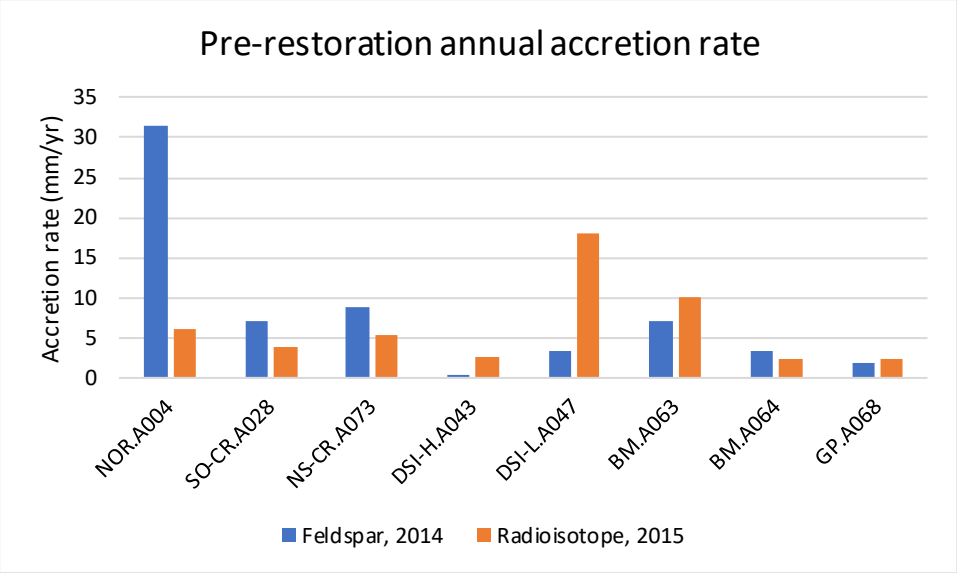

Figure 15. Comparison of annual accretion rates during the pre-restoration period from feldspar marker horizon plots (2014) versus carbon cores (2015), at SFC and reference site locations.

Despite their differences, both methods have their merits. The radioisotope method is an accepted standard for evaluating long-term sediment and carbon accumulation. Deep cores analyzed using this method integrate data across century-long time scales, whereas feldspar marker horizon results may be strongly affected by short-term variability in deposition rates. In its favor, the feldspar marker horizon method is much less time-consuming and less costly compared to radioisotope methods, so more locations can be sampled. Also, the feldspar method may be more useful in evaluating sea level rise

resilience of tidal wetlands, because plants grow on the newly formed, uncompacted sediments measured by the feldspar method, and their establishment and survival is probably little affected by the compaction that occurs at depth. However, as described above, the feldspar method often did not work well in the tall, coarse reed canarygrass-dominated vegetation at the SFC site during the pre-restoration and early post-restoration period, so it has limitations for measuring accretion in such vegetation types.

Significance

This study and other recent reports by our team (Brophy et al. 2017, Peck 2017) provide the first published data on carbon stocks and carbon sequestration in Oregon tidal wetlands, helping to fill a major data gap. Data on carbon sequestration in the Pacific Northwest are very sparse (Cornu 2017) and were previously completely lacking for Oregon. Although a recent, widely-cited project (Crooks et al. 2014) provided solid blue carbon data for one Pacific Northwest estuary in Puget Sound (the Snohomish), the Oregon coast is very different from Puget Sound, so this study provides critical new information needed by land managers, policymakers, and scientists.

The results of this study offer hope for climate change resilience in Tillamook Bay's tidal wetlands. The accretion rates calculated from carbon cores and feldspar plots in least-disturbed high marsh and scrub-shrub tidal swamp exceeds past sea level rise – in other words, to date, these wetlands are keeping pace with sea level rise. Further, the rapid long-term sediment accretion rates observed within the low marsh carbon cores suggest the system has considerable capacity to equilibrate with accelerated future sea level rise. Factors that add to the potential for climate change resilience in Tillamook Bay tidal wetlands include the Bay's high sediment supply (Komar et al. 2004); and fact that the estuary's rivers are undammed, so their sediment transport regimes are largely intact. Due to these factors, Tillamook Bay tidal wetlands -- both least-disturbed wetlands and restoration sites -- may be more resistant to drowning under future, accelerated sea level rise compared to watersheds and wetlands with lower sediment supply and more disturbed watersheds. However, as described above, tidal wetlands can be vulnerable to drowning if the rate of sea level rise exceeds the available sediment supply.

This study indicates high capacity for carbon storage in restored tidal wetlands of the Tillamook Bay estuary. Diking of the SFC site caused an estimated loss of 27,000 tons C_{org} (equivalent to 100,000 tons CO_2). After restoration, we expect that these large carbon losses will be reversed, as the SFC site stores equally large quantities of organic carbon in its soil. Furthermore, restoration of the SFC site will allow future carbon burial at a greater rate under future accelerated sea level rise. However, carbon storage could be reduced if the rate of sea level rise exceeds the available sediment supply, leading to drowning of tidal wetlands and their conversion to mudflats or open water, as described above.

Though sea level rise to date is minor in the Pacific Northwest and human influences have been limited in comparison to East and Gulf Coast tidal wetlands, removal of dikes and wetland restoration are important because Oregon estuaries have limited opportunity for landward migration in response to sea level rise (Brophy and Ewald 2017, Thorne et al. 2018). As sea level rises, healthy tidal wetlands respond by growing both vertically and horizontally (often landward). In the Tillamook Bay estuary, land surfaces at appropriate elevations are available for landward migration, but some of these land surfaces are developed and therefore unsuitable for future tidal wetlands (Brophy and Ewald 2017). In many other Oregon estuaries, the Coast Range prevents much landward migration. Because of these limitations to landward migration, vertical accretion (equilibration of the wetland surface with rising sea levels) is

critical to wetland survival. Reducing human pressure on wetlands through restoration will improve the chances of their survival and the maintenance of their valued ecosystem services.

Lessons learned

Data collected at the reference sites were vital to this project, as they allowed us to estimate the mass of carbon lost after diking; predict the mass of carbon that could be stored following restoration; assess the vulnerability of Tillamook Bay tidal wetlands to drowning under accelerated sea level rise; understand the carbon sequestration functions of least-disturbed Pacific Northwest tidal wetlands; and compare rates of carbon sequestration within the Pacific Northwest to global values.

The large variability in recent sediment accumulation and carbon sequestration values within the SFC site suggests significant within-site heterogeneity. We recommend future studies increase the number of samples within the restoration site to improve our understanding of the deposition patterns across this large site and better understand the variability observed.

The methods used here allowed us to answer important questions about Tillamook Bay least-disturbed and disturbed tidal wetlands. The CT scans allowed us to more easily calculate soil bulk density and observe sedimentary and biological structures. Although the ^{210}Pb method is not commonly used in diked former tidal wetlands, it appeared to produce reliable sediment accretion rates at the diked SFC site, and could therefore be used in future studies of diked sites. The ^{137}Cs method allowed determination of sediment and carbon sequestration rates for rapidly-accreting cores where the ^{210}Pb method did not work, so both methods were needed to obtain good results in this study. The formula derived for converting soil organic matter content to elemental carbon content of the soil is appropriate for use in other northern Oregon tidal wetlands.

References

Allen, J.R.L. 1990. Salt-marsh growth and stratification: A numerical model with special reference to the Severn Estuary, southwest Britain. Marine Geology 95: 77-96.

Brophy, L.S. 2009. Effectiveness Monitoring at Tidal Wetland Restoration and Reference Sites in the Siuslaw River Estuary: A Tidal Swamp Focus. Prepared for Ecotrust, Portland, OR. Green Point Consulting, Corvallis, OR. 125pp. Accessed 1/3/13 at http://hdl.handle.net/1957/35621.

Brophy, L.S., L.A. Brown, M.J. Ewald, and E.K. Peck. 2017. Baseline monitoring at Wallooskee-Youngs restoration site, 2015, Part 2: Blue carbon, ecosystem drivers and biotic responses. Corvallis, Oregon: Institute for Applied Ecology.

Brophy, L.S., C.E. Cornu, P.R. Adamus, J.A. Christy, A. Gray, M.A. MacClellan, J.A. Doumbia, and R.L. Tully. 2011. New tools for tidal wetland restoration: Development of a reference conditions database and a temperature sensor method for detecting tidal inundation in least-disturbed tidal wetlands of Oregon, USA. Report to the Cooperative Institute for Coastal and Estuarine Environmental Technology (CICEET), Durham, NH. 199 pp. Accessed 11/8/16 at http://oregonexplorer.info/data_files/OE_topic/wetlands/documents/01_Brophy_Cornu_CICEET_FINAL_complete_30-Aug-2011.pdf.

Brophy, L.S., and M.J. Ewald. 2017. Modeling sea level rise impacts to Oregon's tidal wetlands: Maps and prioritization tools to help plan for habitat conservation into the future. Prepared for the MidCoast Watersheds Council, Newport, Oregon, USA. Corvallis, Oregon: Institute for Applied Ecology. Accessed 3/3/18 at http://www.midcoastwatersheds.org/s/Modeling-SLR-impacts-to-Oregon-tidal-wetlands-12_1_2017.pdf.

Brophy, L.S., and S. van de Wetering. 2014. Southern Flow Corridor Project effectiveness monitoring plan. Corvallis, Oregon: Institute for Applied Ecology and Confederated Tribes of Siletz Indians. 28p. Accessed 12/21/17 at https://ossfc.files.wordpress.com/2014/01/sfc_effectiveness_monitoring_plan_final_2014-01-07_rev1.pdf

Brown, L.A., M.J. Ewald, L.S. Brophy, and S. van de Wetering. 2016. Southern Flow Corridor baseline effectiveness monitoring: 2014. Corvallis, Oregon: Estuary Technical Group, Institute for Applied Ecology. Prepared for Tillamook County, Oregon. Accessed 3/3/18 at https://ossfc.files.wordpress.com/2013/12/sfc_2014_baseline_em_rev2.pdf.

Cahoon, D. R., J. C. Lynch, and R. M. Knaus. 1996. Improved cryogenic coring device for sampling wetland soils. Journal of Sedimentary Research 66:1025-1027.

Cahoon, D.R., P.E. Marin, B.K. Black and J.C. Lynch. 2000. A method for measuring vertical accretion, elevation, and compaction of soft, shallow-water sediments. Journal of Sedimentary Research. Vol. 70, No. 5. pp. 1250-1253.

Cahoon, D.R., and R.E. Turner. 1989. Accretion and canal impacts in a rapidly subsiding wetland II. Feldspar Marker Horizon Technique. Estuaries 12(4): 260-268.

Callaway, J.C., D.R. Cahoon, and J.C. Lynch. 2013. The surface elevation table–marker horizon method for measuring wetland accretion and elevation dynamics. In Methods in Biogeochemistry of Wetlands. R.D. DeLaune, K.R. Reddy, C.J. Richardson, and J.P. Megonigal, editors. Soil Sci. Soc. Am. Book Series, no. 10.

Chmura, G. L., S.C. Anisfeld, D.R. Cahoon, and J.C. Lynch. 2003. Global carbon sequestration in tidal, saline wetland soils. Global biogeochemical cycles, 17(4).

Cornu, C.E. 2017. Enhancing coastal zone management through quantification and public dissemination of carbon stocks data for Pacific Northwest tidal wetlands. Project Fact Sheet, NOAA Office for Coastal Management, National Estuarine Research Reserve System Science Collaborative. Accessed 3/25/18 at http://graham.umich.edu/activity/35492.

Craft, C.B., E.D. Seneca, and S.W. Broome. 1991. Loss on ignition and Kjeldahl digestion for estimating organic carbon and total nitrogen in estuarine marsh soils: calibration with dry combustion. Estuaries and Coasts 14: 175-179.

Crooks, S., J. Rybczyk, K. O'Connell, D.L. Devier, K. Poppe, and S. Emmett-Mattox. 2014. Coastal blue carbon opportunity assessment for the Snohomish Estuary: The climate benefits of estuary restoration. Report by Environmental Science Associates, Western Washington University, EarthCorps, and Restore America's Estuaries.

Darby, H.C. 1983. The Changing Fenland. Cambridge University Press, London. 267 pp.

Dicken, S.N. 1961. Some recent physical changes of the Oregon coast. Report for the Office of Naval Research, U.S. Department of the Navy, Contract Nonr-2771(04). Department of Geography, University of Oregon.

Diefenderfer, H.L., A.B. Borde, and V.I. Cullinan. 2013. A Synthesis of Environmental and Plant Community Data for Tidal Wetland Restoration Planning in the Lower Columbia River and Estuary. PNNL-22667, prepared by the Pacific Northwest National Laboratory, Marine Sciences Laboratory, Sequim, Washington, for the U.S. Army Corps of Engineers, Portland District, Portland, Oregon.

Ewald, M.J., and Brophy, L.S. 2012. Tidal wetland prioritization for the Tillamook Bay estuary. Prepared for the Tillamook Estuaries Partnership, Garibaldi, OR. Estuary Technical Group of the Institute for Applied Ecology and Green Point Consulting, Corvallis, OR. 123 pp. Accessed 3/24/18 at http://www.tbnep.org/reports-publications/tidal-wetland-prioritization-for-the-tillamook-bay-estuary-2012.pdf

Frenkel, R. E. and J. C. Morlan. 1990. Restoration of the Salmon River salt marshes: Retrospect and prospect. Department of Geosciences, Oregon State University, Corvallis, OR.

Frenkel, R. E. and J. C. Morlan. 1991. Can we restore our salt marshes? Lessons from the Salmon River, Oregon. *The Northwest Environmental Journal*, 7:119-135. Accessed 11/25/12 at http://andrewsforest.oregonstate.edu/pubs/pdf/pub1273.pdf

Hawes, S.M., J.A. Hiebler, E.M. Nielsen, C.W. Alton, J. A. Christy and P. Benner. 2008. Historical vegetation of the Pacific Coast, Oregon, 1855-1910. ArcMap shapefile, Version 2008_03. Oregon Natural Heritage Information Center, Oregon State University. Accessed 12/28/17 at http://www.pdx.edu/sites/www.pdx.edu.pnwlamp/files/glo_coast_2008_03.zip.

Heiri, O., A.F. Lotter and G. Lemcke. 2001. Loss on ignition as a method for estimating organic and carbonate content in sediments: reproducibility and comparability of results. Journal of paleolimnology, 25(1): 101-110.

Howard, J., S. Hoyt, K. Isensee, M. Telszewski, and E. Pidgeon. 2014. Coastal blue carbon: methods for assessing carbon stocks and emissions factors in mangroves, tidal salt marshes, and seagrasses.

Hutchinson, J.N. 1980. The record of peat wastage in the East Anglian fenlands at Holme Post, 1848-1978 A.D. Journal of Ecology 68: 229-249.

IPCC (Intergovernmental Panel on Climate Change). 2014. Climate Change 2014: Synthesis Report. Contribution of Working Groups I, II and III to the Fifth Assessment Report of the Intergovernmental Panel on Climate. Pachauri, R.K., and L.A. Meyer, eds. IPCC, Geneva, Switzerland.

Janousek, C.N., and C.L. Folger. 2014. Variation in tidal wetland plant diversity and composition within and among coastal estuaries: assessing the relative importance of environmental gradients. Journal of Vegetation Science 25: 534–545.

Kauffman, J.B. and D.C. Donato. 2012. Protocols for the measurement, monitoring and reporting of structure, biomass and carbon stocks in mangrove forests. Working Paper 86. CIFOR, Bogor, Indonesia.

Kirwan, M.L., G.R. Guntenspergen, A. D'Alpaos, J.T. Morris, S.M. Mudd, and S. Temmerman. 2010. Limits on the adaptability of coastal marshes to rising sea level. Geophysical Research Letters 37: L23401.

Kirwan, M.L., and J.P. Megonigal. 2013. Tidal wetland stability in the face of human impacts and sea-level rise. Nature, 504(7478): 53-60.

Kirwan, M.L., S. Temmerman, E.E. Skeehan, G.R. Guntenspergen, and S. Fagherazzi. 2016. Overestimation of marsh vulnerability to sea level rise. Nature Climate Change 6: 253-260.

Komar, P.D., J.C. Allan, and P. Ruggiero. 2011. Sea level variations along the US Pacific Northwest coast: Tectonic and climate controls. Journal of Coastal Research, 27(5): 808-823.

Komar, P. D., J. McManus, and M. Styllas. 2004. Sediment accumulation in Tillamook Bay, Oregon: natural processes versus human impacts. The Journal of Geology, 112(4): 455-469.

Levesque, P. 2013. A history of the Oregon Solutions Southern Flow Corridor Project – Landowner Preferred Alternative, a review of the alternatives and a summary of public involvement. Tillamook County, Oregon. Accessed 12/27/17 at https://ossfc.files.wordpress.com/2014/05/b_white-paper.pdf.

Mcleod, E., G.L. Chmura, S. Bouillon, R. Salm, M. Björk, C.M. Duarte, C.E. Lovelock, W.H. Schlesinger, and B.R. Silliman. 2011. A blueprint for blue carbon: toward an improved understanding of the role of vegetated coastal habitats in sequestering CO_2. Frontiers in Ecology and the Environment, 9(10): 552-560.

Morris, J.T., P.V. Sundareshwar, C.T. Nietch, B. Kjerfve and D. R. Cahoon. 2002. Responses of coastal wetlands to rising sea level. Ecology 83: 2869-2877.

Morris, J.T., and G.J. Whiting. 1986. Emission of gaseous carbon dioxide from salt-marsh sediments and its relation to other carbon losses. Estuaries and Coasts 9: 9-19.

NHC (Northwest Hydraulic Consultants) and HBH Consulting Engineers. 2010. Project Exodus Final Report. Prepared for Oregon Solutions Design Team and Tillamook County.

Pearson, M.L. 2002. Fluvial geomorphic analysis of the Tillamook Bay Basin rivers. Report to Portland District, U.S. Army Corps of Engineers and Tillamook County, Oregon. Bohica Ent., Monmouth, OR.

Peck, E.K. 2017. Competing roles of sea level rise and sediment supply on sediment accretion and carbon burial in tidal wetlands; Northern Oregon, U.S.A. M.S. Thesis, Oregon State University. Accessed 3/25/18 at http://ir.library.oregonstate.edu/xmlui/handle/1957/61372.

Phillip Williams and Associates. 2002. Tillamook Bay integrated river management strategy. Report to U.S. Fish and Wildlife Service, U.S. Environmental Protection Agency, and U.S. Army Corps of Engineers. Phillip Williams and Associates, Corte Madera, CA.

Roegner, G.C., H.L. Diefenderfer, A.B. Borde, R.M. Thom, E.M. Dawley, A.H. Whiting, S.A. Zimmerman, and G.E. Johnson. 2008. Protocols for monitoring habitat restoration projects in the lower Columbia River and estuary. PNNL-15793. Report by Pacific Northwest National Laboratory, National Marine Fisheries Service, and Columbia River Estuary Study Taskforce submitted to the U.S. Army Corps of Engineers, Portland District, Portland, Oregon.

Simenstad, C.A., C.D. Tanner, R.M. Thom, and L. Conquest. 1991. Estuarine habitat assessment protocol. UW-FRI-8918/-8919 (EPA 910/9-91-037), Rep. to U.S. Environ. Protect. Agency - Region 10. Wetland Ecosystem Team, Fish. Res. Inst., Univ. Wash., Seattle, WA. 191 pp., Appendices.

Simenstad, C.A., and R.M. Thom. 1996. Functional Equivalency Trajectories of the Restored Gog-Le-Hi-Te Estuarine Wetland. Ecological Applications 6(1): 38. Accessed 3/24/18 at http://www.tidalmarshmonitoring.org/pdf/Simenstead1996_RestorationTrajectory.pdf.

Thom, R.M. 1992. Accretion rates of low intertidal salt marshes in the Pacific Northwest. Wetlands 12: 147-156.

Thorne, K., G. MacDonald, G. Guntenspergen, R. Ambrose, K. Buffington, B. Dugger, C. Freeman, C. Janousek, L. Brown, J. Rosencranz, J. Holmquist, J. Smol, K. Hargan, and J. Takekawa. 2018. U.S. Pacific coastal wetland resilience and vulnerability to sea-level rise. Science Advances 21 Feb 2018 : eaao3270. Accessed 3/24/18 at http://advances.sciencemag.org/content/4/2/eaao3270.full.

Tillamook County. 2013. Southern Flow Corridor-landowner preferred alternative: FY 2013 coastal and marine habitat restoration project grant application.

U.S. EPA (U.S. Environmental Protection Agency). 2018. Greenhouse gas equivalency calculator. Accessed 12/28/18 at https://www.epa.gov/energy/greenhouse-gas-equivalencies-calculator.

Wheatcroft, R. A., M.A. Goñi, K.N. Richardson, and J.C. Borgeld. 2013. Natural and human impacts on centennial sediment accumulation patterns on the Umpqua River margin, Oregon. Marine Geology, 339: 44-56.

Wheatcroft, R. A. and C. K. Sommerfield. 2005. River sediment flux and shelf sediment accumulation rates on the Pacific Northwest margin. Continental Shelf Research, 25(3): 311-332.

Williams, M. 1970. The draining of the Somerset Levels. Cambridge University Press, London. 288 pp.

Appendix 1. Maps

List of maps:

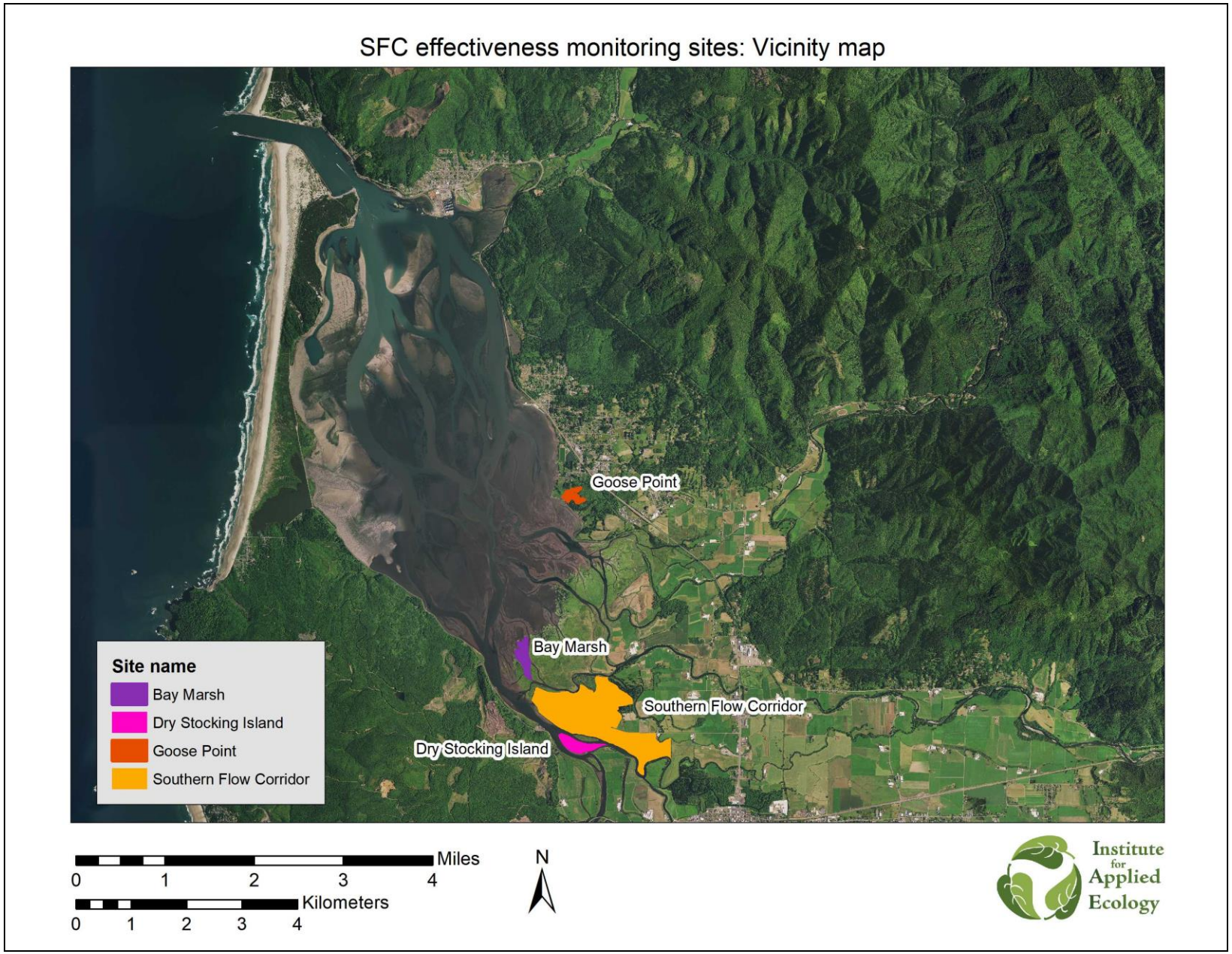

Map 1. Vicinity map of Tillamook Bay estuary and SFC effectiveness monitoring sites. Monitoring sites are described in the SFC Effectiveness Monitoring Plan (Brophy and van de Wetering 2014). Background image: NAIP 2014.

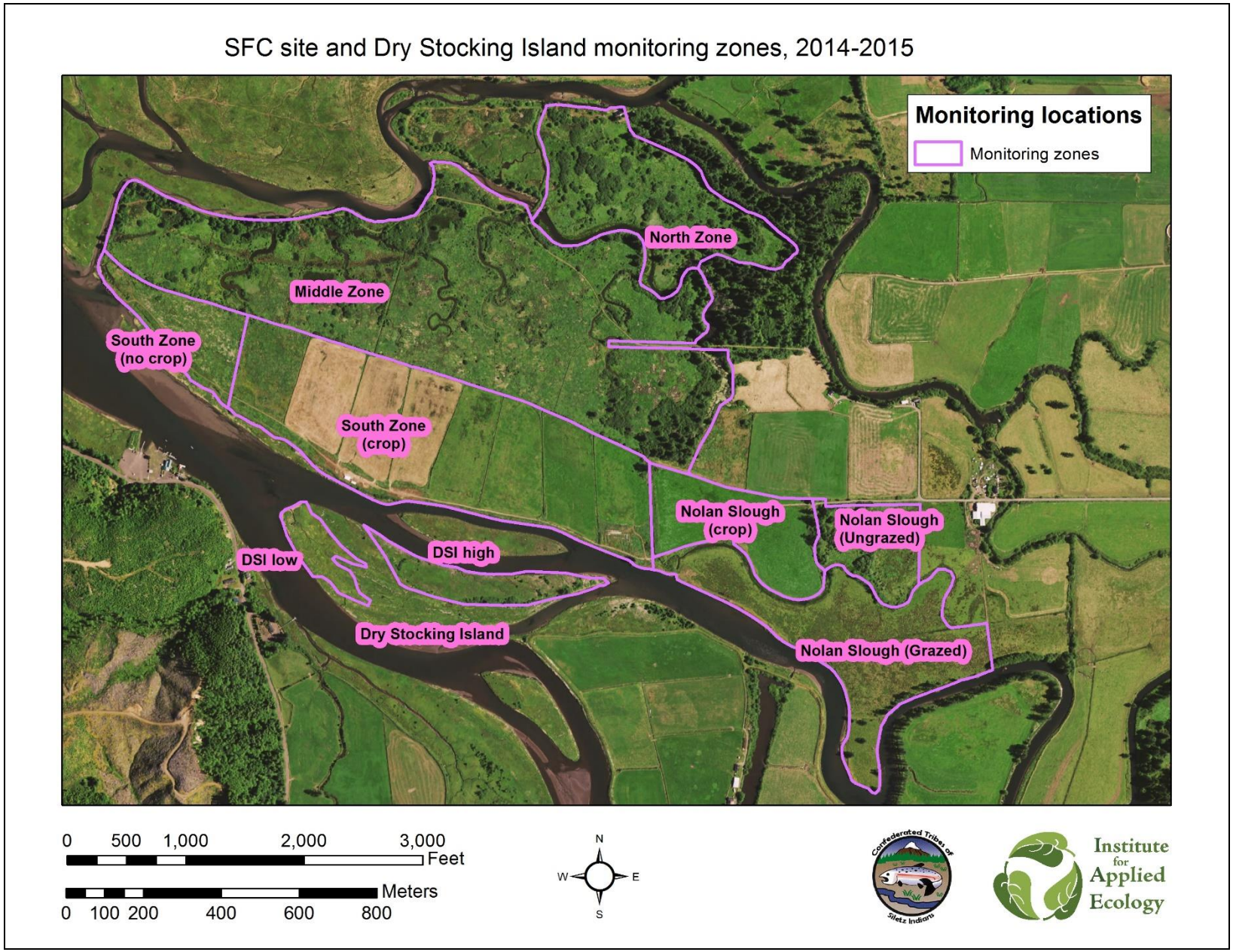

Map 2. Monitoring zones at the SFC site and Dry Stocking Island reference site. Monitoring zones are described in the SFC Effectiveness Monitoring Plan (Brophy and van de Wetering 2014). Background image: NAIP 2014.

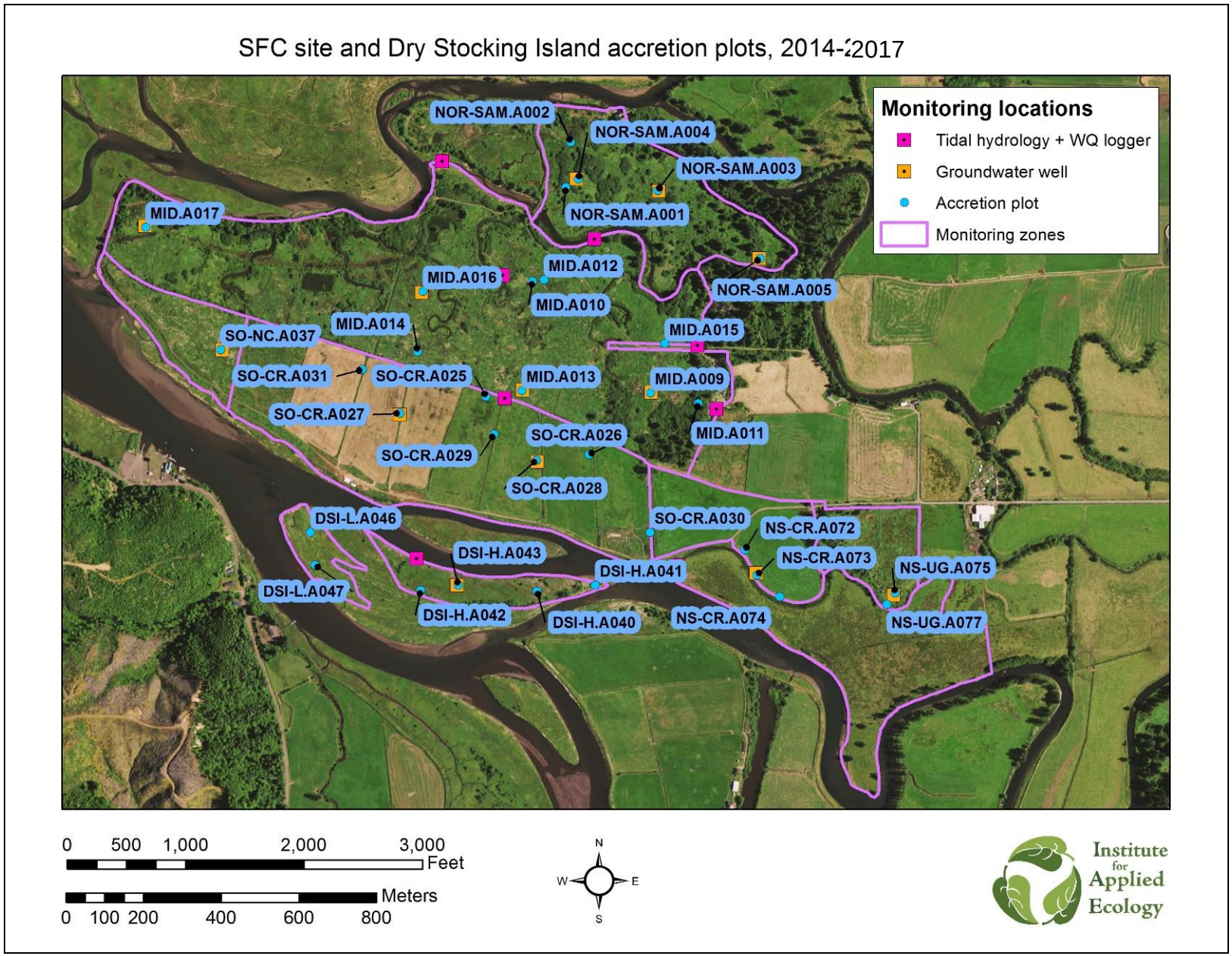

Map 3. Sediment accretion plots sampled during 2014-2017 at the SFC site and Dry Stocking Island (DSI) reference site (blue dots). Not all locations were sampled in 2017; see Table 1 above. Monitoring zones (pink outlines) are described in the SFC Effectiveness Monitoring Plan (Brophy and van de Wetering 2014). Background image: NAIP 2014.

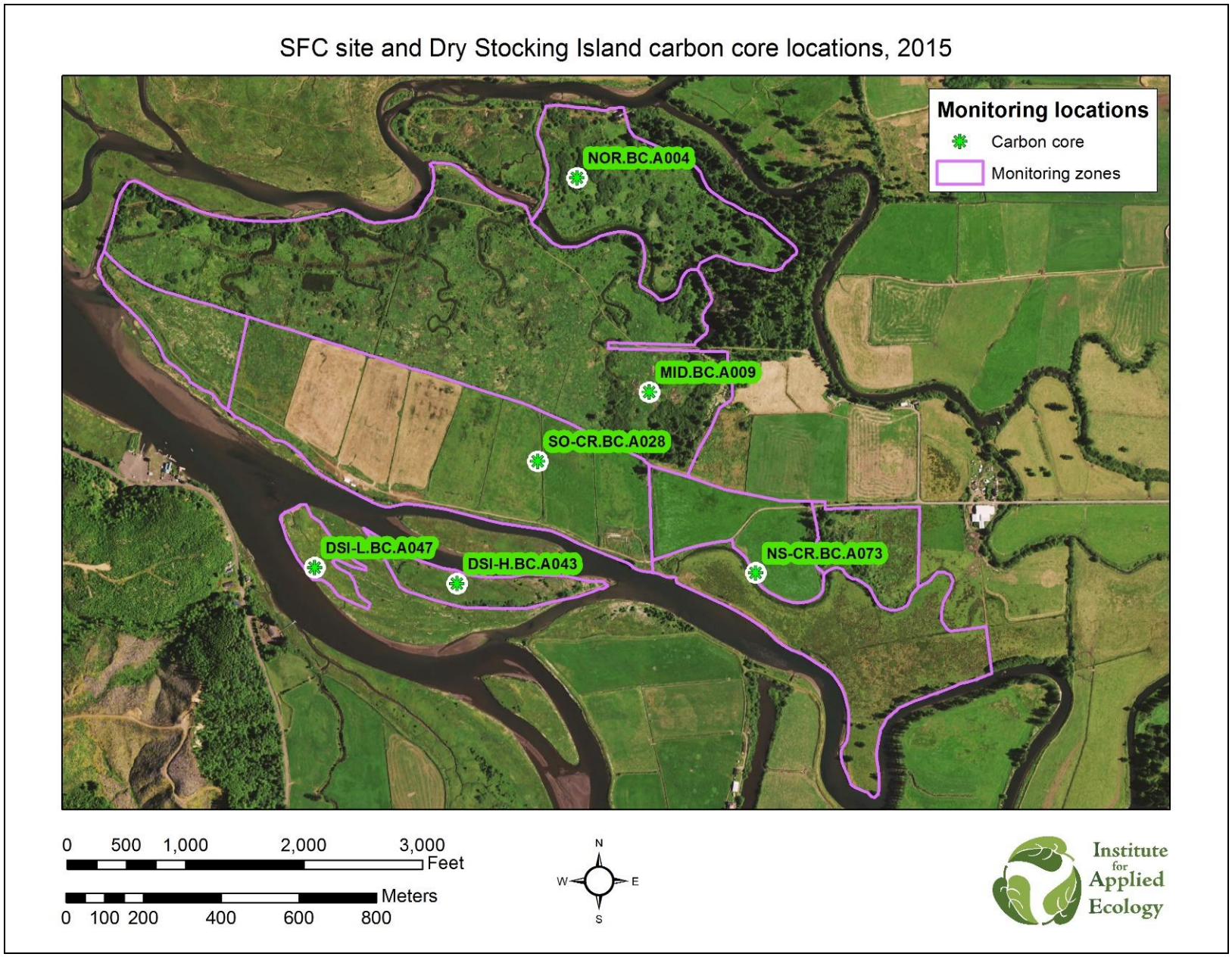

Map 4. Carbon core locations in 2015 at the SFC site and Dry Stocking Island (DSI) reference site. Monitoring zones (pink outlines) are described in the SFC Effectiveness Monitoring Plan (Brophy and van de Wetering 2014). Background image: NAIP 2014.

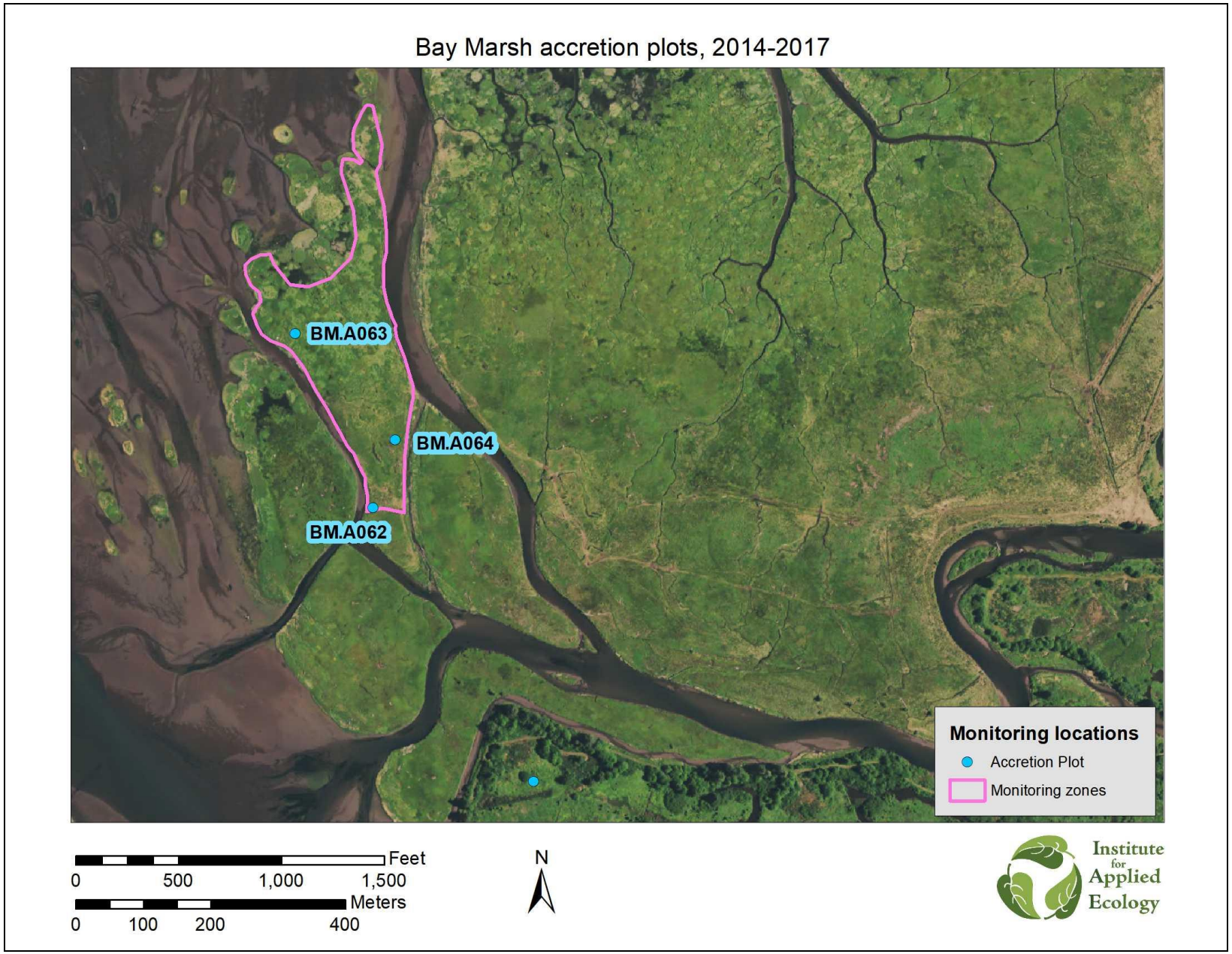

Map 5. Sediment accretion plots sampled 2014-2017 at the Bay Marsh reference site. Monitoring zones (pink outlines) are described in the SFC Effectiveness Monitoring Plan (Brophy and van de Wetering 2014). Background image: NAIP 2014.

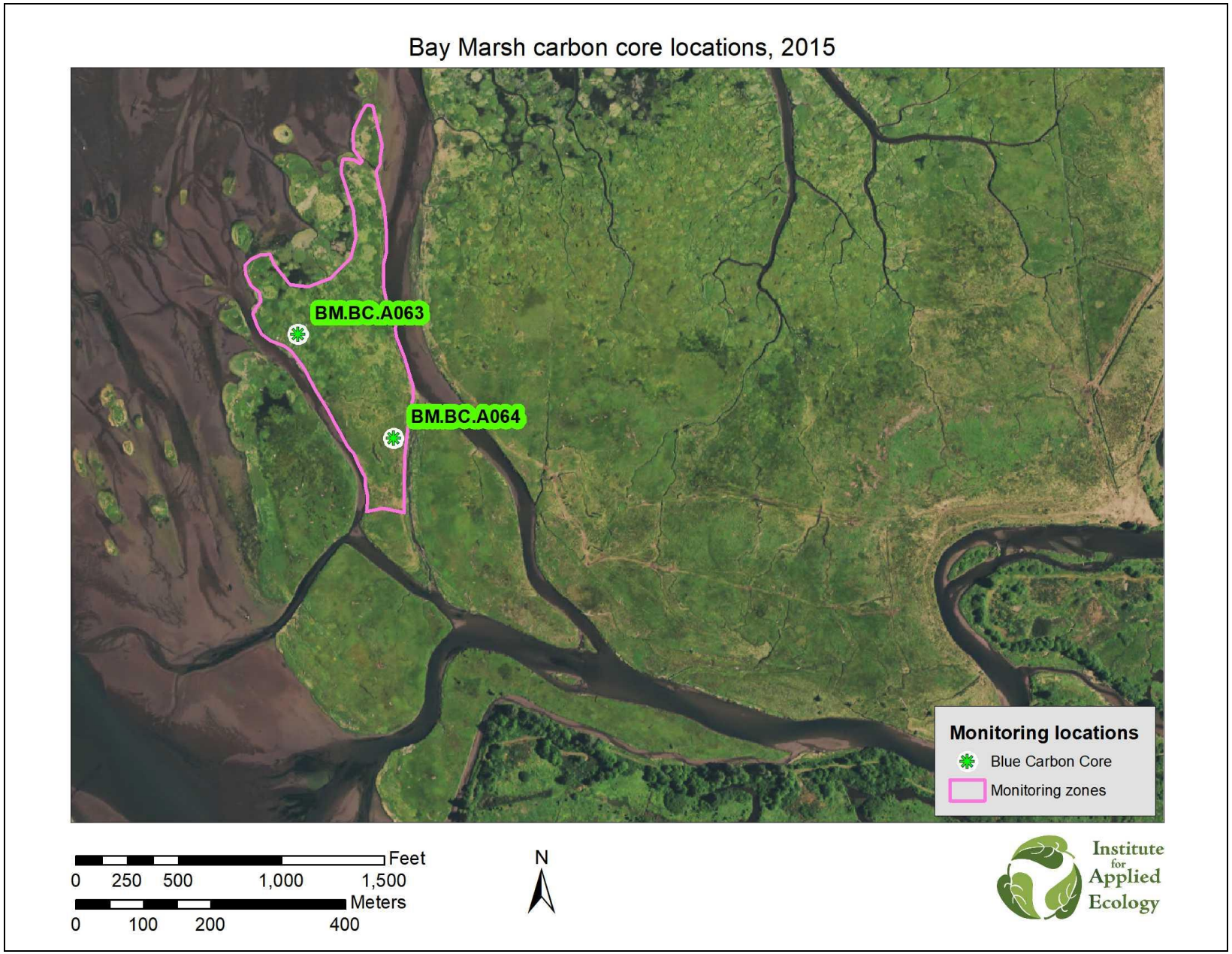

Map 6. Carbon core locations in 2015 at the Bay Marsh reference site. Monitoring zones (pink outlines) are described in the SFC Effectiveness Monitoring Plan (Brophy and van de Wetering 2014). Background image: NAIP 2014.

Map 7. Sediment accretion plots sampled 2014-2017 at the Goose Point reference site. Monitoring zones (pink outlines) are described in the SFC Effectiveness Monitoring Plan (Brophy and van de Wetering 2014). Background image: NAIP 2014.

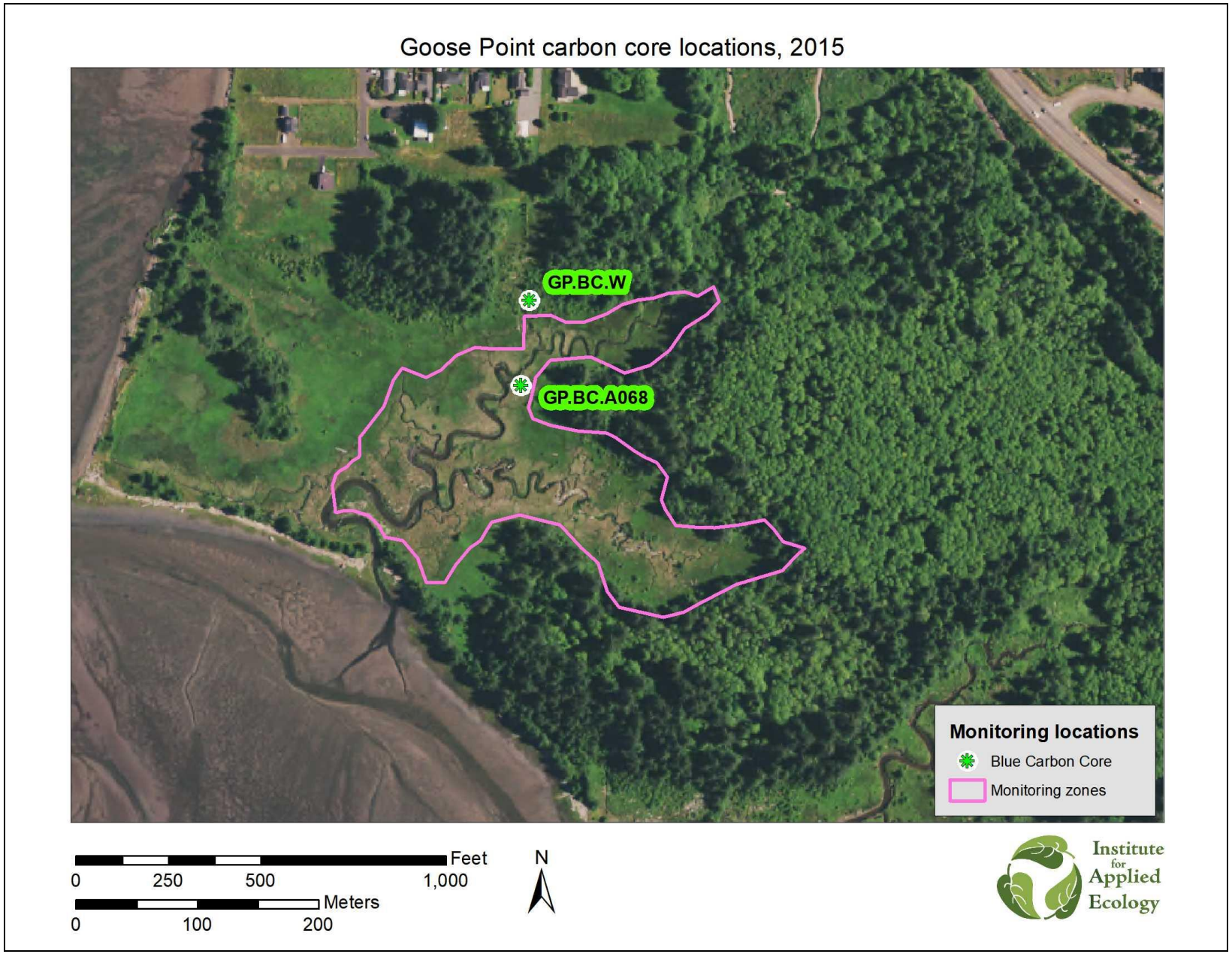

Map 8. Carbon core locations in 2015 at the Goose Point reference site. Monitoring zones (pink outlines) are described in the SFC Effectiveness Monitoring Plan (Brophy and van de Wetering 2014). Background image: NAIP 2014.

Appendix 2. Spatial reference system and spatial data accuracy

GPS data and map products for this project used the spatial reference system described in the table below.

Horizontal and vertical coordinate systems for ETG-collected GPS data

Horizontal Coordinate System	Universal Transverse Mercator (UTM) Zone 10 North
Horizontal Datum	North American Datum of 1983 (NAD83) Adjustment 2011 Epoch 2010.00
Vertical Datum	North American Vertical Datum of 1988 (NAVD88)
Geoid model	NGS Geoid 12A
Units	Meters

GPS/GNSS methods

Data was collected using a Spectra Precision ProMark 220 GNSS receiver outfitted with an Ashtech ASH111661 external GNSS antenna. The receiver collected both GPS and GLONASS L1/L2 signals at 1 Hz and received real-time kinematic corrections (RTK) from the Oregon Realtime GNSS Network (ORGN, http://theorgn.net) using a cellular data link. The receiver and antenna were mounted on an aluminum survey rod that was manually leveled or stabilized with a bipod during collection. The bottom of the survey rod was fitted with an 11 cm diameter topo shoe to prevent the survey rod from penetrating soft soil and mud. Typical occupation durations were 10 seconds for general ground surface measurements. Local benchmarks and measurements of survey control had a typical occupation time of 240 seconds or greater.

Spatial data accuracy

Spatial data accuracy was calculated for each field campaign associated with this project following the National Standard for Spatial Data Accuracy (NSSDA) and repeated measurements of published NGS benchmarks near the project area. Typical absolute accuracies were 3.5 cm horizontal and 5.0 cm vertical at the 95% confidence level. Please contact the lead author for more information.

Feet / meters conversion

All analyses were performed in meters and converted to feet when necessary for reporting. The conversion used the International Foot, which is equal to exactly 0.3048 m.